DETERMINING THE DIFFERENTIAL ROLES OF THE DOCK FAMILY OF GEFS IN *DROSOPHILA* DEVELOPMENT

A DISSERTATION IN

Cell Biology & Biophysics

and

Molecular Biology & Biochemistry

Presented to the Faculty of the University
of Missouri-Kansas City in partial fulfillment of
the requirements for the degree

DOCTOR OF PHILOSOPHY

by

BRIDGET H. BIERSMITH

B.S. Biology, University of Missouri – Kansas City, 2009

Kansas City, Missouri

2014

DETERMINING THE DIFFERENTIAL ROLES OF THE DOCK FAMILY OF GEFS IN *DROSOPHILA* DEVELOPMENT

Bridget Hope Biersmith, Candidate for the Doctor of Philosophy Degree

University of Missouri - Kansas City, 2014

ABSTRACT

The evolutionarily conserved Dock proteins function as unconventional guanine nucleotide exchange factors (GEFs). Upon binding to ELMO (Engulfment and cell motility) proteins, Dock-ELMO complexes activate the Rho family of small GTPases to mediate a diverse array of biological processes, including cell motility, apoptotic cell clearance, and axon guidance. Overlapping expression patterns and functional redundancy among the eleven vertebrate Dock family members, which are subdivided into four families (Dock-A, B, C, and D), complicate genetic analysis. *Drosophila melanogaster* is an excellent genetic model organism to understand Dock protein function as its genome encodes one ortholog per subfamily: Myoblast city (Mbc; Dock-A) and Sponge (Spg; Dock-B). The target GTPase of the Dock-A subfamily is Rac, which modulates actin dynamics. However, the *in vivo* GTPase downstream of the Dock-B subfamily remains unclear. Herein we show that the roles of Spg and Mbc are not redundant in the *Drosophila* somatic muscle, central nervous system (CNS), or the dorsal vessel (dv). Moreover, we confirm the *in vivo* role of Mbc upstream of Rac and provide evidence that Spg functions in concert with Rap1 to regulate aspects of adhesion. Together these data show that Mbc and Spg can have differential downstream GTPase targets. Our findings predict that the ability to regulate downstream GTPases is

dependent on cellular context and allows for the fine-tuning of actin cytoskeletal or cell adhesion events in biological processes that undergo cell morphogenesis.

APPROVAL PAGE

The faculty listed below, appointed by the Dean of the School of Graduate Studies have examined a dissertation titled "Determining the Differential Roles of the Dock Family of GEFs in *Drosophila* Development" presented by Bridget H. Biersmith, candidate for the Doctor of Philosophy degree, and certify that in their opinion it is worthy of acceptance.

Supervisory Committee

Erika R. Geisbrecht, Ph.D., Committee Chair
Department of Cell Biology & Biophysics

Samuel Bouyain, Ph.D.
Department of Molecular Biology & Biochemistry

Leonard L. Dobens, Ph.D.
Department of Molecular Biology & Biophysics

Alexander Idnurm, Ph.D.
Department of Cell Biology & Biophysics

Jeffery Price, Ph.D.
Department of Molecular Biology & Biochemistry

CONTENTS

TABLES

ILLUSTRATIONS

ACKNOWLEDGMENTS

The authors would like to thank Susan Abmayr, Pernille Rorth, Eyal Schejter, Chi-Hon Lee, and Thomas Clandinin for providing fly stocks and reagents. We are grateful to Susan Abmayr, in whose lab this project was initiated. We thank the Developmental Studies Hybridoma Bank developed under NICHD for antibodies and the Bloomington Stock Center for flies. We also thank Len Dobens for helpful discussion.

The authors would also like to thank Masa Yamaguchi for providing fly stocks and reagents. We would like to thank Zong-Heng Wang, Nicole Green, and Jessica Kawakami for careful reading of this manuscript. We thank the Developmental Studies Hybridoma Bank developed under NICHD for antibodies and the Bloomington Stock Center for flies. We also thank Len Dobens, Richard Cripps, Susan Abmayr, Achim Pauluat, and Sunita Kramer for helpful discussion. Finally, we would like to thank the St. Louis University Research Core and Histology Services as well as members of the University of Missouri – Kansas City Histology Core, especially Leanne Szerzen and Doug Law, to whose memory this manuscript is dedicated. This work was supported by a Predoctoral Fellowship from the American Heart Association Midwest Affiliate (12PRE12050380) to B.H.B and NIH RO1AR060788 to E.R.G.

CHAPTER 1

INTRODUCTION

Rho GTPases are enzymes that bind and hydrolyze GTP, allowing for physical interactions with downstream proteins to activate pathways involved in cell morphogenesis, including cell migration, cell adhesion, and phagocytosis[1, 2]. Normal development and tissue homeostasis requires proper regulation of the GTP hydrolysis cycle to tightly control cytoskeletal cell shape changes and cell-cell adhesion events[3]. Inappropriate control of cell morphogenesis can manifest in abnormal cellular behaviors. For example, during tumor metastasis, cancerous cells may detach from their original location, undergo cytoskeletal rearrangement and alter membrane adhesion dynamics in order to migrate through the complex extracellular environment. Many of the same molecules are essential for cell morphogenetic events in normal or abnormal cells[4]. This allows us to determine the normal function of proteins that control GTPases and extrapolate how abnormal misregulation may result in genetic birth defects or disease progression in different biological contexts.

The Rho GTPases are key regulators in cell morphogenesis, constantly cycling between an "off" and an "on" state. GTPase Activating Proteins (GAPs) facilitate the exchange of GTP for GDP to inactivate GTPases. Counteracting this, GEFs assist in the exchange of GDP for GTP, turning on the GTPase and allowing it to bind to downstream effectors. GDP exchange of Rho GTPases is facilitated by two types of GEFs; the Dbl family and the Dock family. Proteins of the Dbl family contains a conserved tandem Dbl homology (DH) and Pleckstrin homology (PH) catalytic sequence[1, 2]. In contrast, the unconventional Dock GEFs lack the canonical DH domain, and instead utilize an internal

Dock homology region 2 (DHR2) for GTPase binding and a separate SH3 domain that interacts with the adaptor protein ELMO, which localizes Dock proteins to specific regions for GTPase activation. Normally, ELMO and Dock exist in an autoinhibitory state in the cytoplasm and, upon stimulation by external cues, can relieve this inhibition, thus allowing the ELMO-Dock complex to be recruited to the membrane to function with downstream GTPsae targets[1].

Recent studies have identified a class of non-canonical GEFS that are members of the CDM (*C. elegans* Ced-5, human DOCK180, *Drosophila* Myoblast city) family of proteins [5, 6]. Evolutionarily conserved, Mbc/DOCK180/Ced-5 proteins contain an N-terminal Src-homology-3 domain (SH3), two internal DOCK-homology regions (DHR-1 and DHR-2), and a C-terminal proline–rich region. The DHR1 regions of both DOCK180 and Mbc bind to phosphatidylinositol 3,4,5-triphosphate [7 7, 8]. Vertebrate cell culture studies show this region is required for membrane localization [7]. In flies, the DHR1 domain is not essential for recruitment to the membrane, but is essential for myoblast fusion as deletion of the DHR1 domain fails to rescue *mbc* mutant embryos in functional rescue assays [8]. Although the SH3-domain containing protein Crk is capable of binding the C-terminal proline-rich region of both DOCK180 and Mbc, it is not always essential *in vivo*. A direct interaction between vertebrate DOCK180 and CrkII is not required for apoptotic cell removal [9]. Furthermore, deletion of the Ced-2/Crk binding sites in *C. elegans* Ced-5/DOCK180 does not affect cell engulfment or migration [9]. Consistent with this, while *Drosophila* Crk binds Mbc, it is dispensable for myoblast fusion [8]. Whereas canonical GEFs contain both typical Dbl-homology domain (DH) and Pleckstrin-homology domains (PH) that are involved in activation of the Rho GTPases,

these domains are absent in CDM family members [6, 7]. Conventional GEFs bind nucleotide-free Rac via their DH domain, while the CDM proteins use the DHR2 region. Deletion or mutation of this domain results in a loss of Rac binding and activation [10, 11]. A DOCK-Rac protein complex is sufficient for Rac activation [7, 12], but may be enhanced by DOCK180 bound to ELMO [10, 13, 14].

ELMO/Ced-12 (hereafter referred to as ELMO) was originally identified in *C. elegans* as an upstream regulator of Rac in apoptotic cell engulfment and cell migration [15]. Studies using mammalian ELMO1 subsequently showed that the DOCK180-ELMO complex is required for Rac-mediated cell migration and phagocytosis [10, 13, 14, 16, 17]. The PH domain, which in conventional GEFs targets protein to the membrane through its interactions with phosphatidylinositol lipids or other protein-protein interactions, is provided by the ELMO protein in the DOCK-ELMO complex [10, 12]. The N-terminal SH3 domain of CDM family members associates with the C-terminal region of the ELMO family of proteins [18]. While the molecular function of ELMO in the DOCK→Rac signaling pathway still needs to be clarified, it is worth noting that ELMO has functions independent of the DOCK proteins.

Importantly, studies in *Drosophila* have provided additional insight into role of the Mbc-ELMO→Rac signaling pathway in multiple tissues. Mutations in *mbc* and *elmo* result in border cell migration defects in the ovary and myoblast fusion defects in the embryo [19-21]. Decreased Mbc and ELMO function exhibit abnormal ommatidial organization in the eye and thorax closure defects in the adult [21, 22]. In addition, loss-of-function studies have demonstrated that the *Rac* genes are required redundantly in a variety of developmental processes, including border cell migration, myoblast fusion, and

axon guidance in the developing nervous system [21, 23, 24]. Last, genetic interactions exist between the atypical GEF Mbc-ELMO complex and their target GTPase Rac. A genetic screen in the eye uncovered an allele of *mbc* that suppresses the Rac1 overexpression phenotype [25]. In support of this, removal of one copy of both *Rac1* and *Rac2* are capable of ameliorating the "activated-Rac" phenotype exhibited by co-expression of both Mbc and ELMO in the eye [21].

There are 11 Dock proteins in mammals that are subdivided into four categories: Dock A-D. To date, Dock-A, -B, and -C family members can all activate the Rho GTPase Rac, while Dock-C and –D proteins also show specificity for Cdc42[1, 2]. Expanding the repertoire of GTPase targets, the Dock-B subgroup member Dock4 has also been shown to activate the Ras-like small GTPase Rap1[26-28]. Dock-A family member, Dock1, is required for vertebrate neuronal pathfinding, endothelial cell migration, and functions in concert with a second Dock-A member, Dock5, in vertebrate muscle development[1, 2]. Less is known about the developmental roles of the DockB family, however both subfamily members, Dock3 and Dock4, are expressed in nervous system tissue, with Dock4 expression also expanding into the muscle[29-31]. While the function of this family in the nervous system is unclear, *Dock3*$^{-/-}$ mice exhibit neuronal degeneration. This result along with several other *in vitro* and over-expression studies indicate a role in axonal outgrowth and/or neuroprotection[2, 32]. Furthermore, a screen using human cancer cell lines identified a single Dock4 point mutation in two different cancer cell lines. This same study showed Dock4-mediated Rap activation was required for cells to maintain their cell-cell adhesion junctions[26].

Redundancy is simplified in flies with only one Dock homolog per subfamily. In *Drosophila*, the Dock-A counterpart, Myoblast City (Mbc), is required for Rac-mediated processes, such as myoblast fusion and border cell migration that require modulation of the actin cytoskeleton[1, 2]. Mbc also functions redundantly with the Dock-B homolog, Sponge (Spg), in border cell migration[33]. However, it is unclear if the two function redundantly in other processes. For instance, Spg is required for proper CNS development and genetically interacts with the adhesion protein N-cadherin in this process, while Mbc does not. These results are not necessarily surprising as *spg* transcript has high expression in the CNS relative to *mbc* transcript, which has higher expression in the somatic muscle. However, both transcripts are expressed in the visceral gut muscle and dorsal vessel (DV), or the *Drosophila* equivalent to the heart[29]. It was also recently shown that Spg is required for Rap-mediated photoreceptor differentiation in the *Drosophila* eye, one of the first *in vivo* examples of this relationship[28].

Herein, we use the genetically tractable model organism *Drosophila melanogaster* to determine if Mbc and Spg function redundantly in tissues other than border cell migration and to establish if these Dock proteins target the same or different GTPases *in vivo*. Using genetic interaction analyses, RNAi knockdown, and rescue experiments with the GAL4/UAS system, we have established that Mbc and Spg have differential functions in the development of the somatic muscle, CNS, and DV. In addition, we show that the downstream GTPases of these GEFs are different in dorsal vessel development. This is one of the first *in vivo* examples of these two closely related proteins having clear and distinct targets in development.

CHAPTER 2

THE DOCK PROTEIN SPONGE BINDS TO ELMO AND FUNCTIONS IN *DROSOPHILA* EMBRYONIC CNS DEVELOPMENT

Identification of the DOCK3 and DOCK4 ortholog CG31048/Sponge as an ELMO-interacting protein

To identify proteins that may interact with ELMO in the developing embryonic musculature, tissue-specific immunoprecipitations (IPs) were carried out as described in Geisbrecht, et al [21]. In brief, either HA-tagged or untagged ELMO, both of which rescue *elmo* mutants, were expressed using the muscle-specific *mef2-GAL4* driver. ELMO-specific complexes were isolated from embryonic lysates with anti-HA resin, digested with trypsin, and analyzed by Multidimensional Protein Identification Technology (MudPIT) mass spectrometry [34]. In an average of 5 independent experiments, the percent peptide coverage of ELMO ranged from 43-73% (Figure 1A), while the most abundant associated protein was Mbc [21]. Peptides corresponding to the protein CG31048 were detected in lysates immunoprecipitated with tagged ELMO, but not untagged ELMO. After Mbc, CG31048 was the second most abundant protein detected, where the percentage of peptide coverage that corresponded to CG30148 ranged from 2-30%. While the *CG31048* cDNA had not yet been cloned, an abstract from the 2005 fly meeting by Eyal Schejter et al., linked this locus to a maternal effect mutant called *sponge* (*spg*), whose name we will use hereafter. An allele of *spg* was originally identified by Rice and Garen [35], while more alleles emerged from screens in the laboratory of C. Nusslein-Volhard. Postner, et al., examined the role of Spg in early actin

cap and metaphase furrow formation in early embryonic development [36]. In addition, the Rorth lab determined that both Mbc and Spg function redundantly in border cell migration downstream of the receptor PVR [37]. However, the role of Spg in later embryonic processes has not been examined.

Spg is most closely related to both mammalian DOCK3/MOCA and DOCK4 and is a CDM family member whose domain structure is highly similar to Mbc (Figure 1B). All of these related proteins contain an N-terminal Src-homology 3 domain (SH3), and internal DOCK homology region-1 (DHR-1) and DOCK homology region-2 (DHR-2) domains. Spg shares greater amino acid sequence identity to vertebrate DOCK3 and DOCK 4 (42% and 40%, respectively) than Mbc (33%). This primary amino acid identity/similarity (33%/52%) between Spg and Mbc decreases to 16% amino acid identity and 21% amino acid in the C-terminal proline-rich region. Notably, the C-terminal region of Spg contains 7 predicted proline rich sites not present in Mbc. This is similar to vertebrate analyses of DOCK family members, where the number of proline-rich sites in the C-terminal region of DOCK3 and DOCK4 is greater than that found in DOCK180 alone [38]. It is hypothesized that this region may confer differential properties of DOCK family function.

To confirm a potential physical interaction between ELMO and CG31048, we generated antisera to the C-terminal region of Spg that is the most divergent from Mbc. Similar to the MS experiments in which Spg was identified, both HA-tagged ELMO and untagged ELMO were expressed in the developing musculature with *mef2-GAL4*. After preparing embryonic lysates, anti-HA beads were used to immunoprecipitate HA-tagged and untagged ELMO. Consistent with results that show both vertebrate DOCK3 and

DOCK4 are associated with ELMO [17, 39], Spg could be visualized in an ELMO-associated complex by immunoblotting with anti-Spg (Figure 1C).

Spg mRNA and protein is strongly expressed in the developing nervous system

Portions of the *spg* transcript were identified in a screen for neural precursor genes [40]. We confirmed this using *in situ* hybridization analysis that revealed *spg mRNA* is expressed strongly in the developing nervous system throughout embryonic development. *In situs* showed *spg mRNA* is detected in the nervous system primordia and sensory neurons in stage 11 and stage 13 embryos (Figure 2A, B). This strong expression persisted in the ventral nerve cord until the end of embryogenesis (Figure 2E, F). Staining in the visceral mesoderm in stage 13 embryos (Figure 2C, arrowheads) confirmed the identification of Spg from our muscle-specific MS analysis as the *mef2-GAL4* driver is expressed in both the visceral and somatic musculature. Similar to *mbc* [20], *spg mRNA* expression was also apparent in the dorsal vessel (Figure 2D, E, arrows). While *mbc* is also expressed abundantly in the developing somatic, or body wall musculature [20], *spg* expression is low or undetectable in this tissue (Figure 2C, solid lines). Thus, *spg* and *mbc* exhibit overlapping RNA expression patterns in the developing visceral musculature and dorsal vessel [20], while they are uniquely expressed in others. Mbc is strong in the somatic musculature, while Spg expression is predominant in the developing nervous system.

To confirm and extend our mRNA expression analysis, we examined the distribution of Spg protein using antisera generated against the C-terminal region of Spg. Consistent with *spg* mRNA expression, Spg protein was detected in the ventral nerve

cord and visceral mesoderm (Figure 2G, H). A ventral view also revealed expression in the peripheral neurons (Figure 2I, arrows). In addition, Spg immunoreactivity was apparent in all longitudinal and commissural neurons (Figures 2J-J''). Spg was not detected in the general population of glial cells by co-staining with the glial cell marker Repo at stage 13 (Figure 2K-K'') or the midline glial cell marker Slit at stage 16 (Figure 2L-L'').

Spg and ELMO are required for development of the central nervous system

All alleles of *spg* isolated in the laboratory of Christian Nüsslein-Volhard and analyzed by the Weischaus lab were homozygous viable and female sterile [36]. Although many of the original alleles were not available for these studies, a stop codon was identified by sequencing the spg^{242} (previously called spg^{2}) allele (W487*). Consistent with Postner, et al. [36], we found that eggs produced from spg^{242} homozygous mothers with a mutant paternal allele of *spg* die early in embryonic development. To confirm that the lethality of *spg* is due to the *spg* locus, we were able to rescue this lethality by driving a *UAS-spg* cDNA with the early *nanos-GAL4* driver (n=208). As maternal *spg* mutants die early and could not be examined for defects in later developmental processes, we examined embryos zygotically mutant for spg^{242}/spg^{242} for defects in nervous system development.

For proper innervation of muscles in development, neurons send out actin-rich growth cones (outgrowth), bundle and unbundle when appropriate (fasciculation), and make decisions to cross the ventral nerve cord (axon guidance). For all experiments that include analysis of axon outgrowth and guidance, Fasciclin II (FasII) was utilized to label

three tracts of longitudinal fascicles that run parallel to the nerve cord. A WT embryo labeled with FasII is shown in Figure 3A. Breaks in the longitudinal fascicles indicate axon stalling or outgrowth defects, while axons that cross the ventral midline are misguided. The global neuropile marker BP102 labels all longitudinal and commissural axons, resulting in a ladder-like appearance of the axonal projections (Figure 3F). Consistent with a maternal contribution of Spg mRNA and protein, embryos homozygous mutant for the spg^{242} allele exhibited minor defects in the axonal patterns. Labeling with FasII revealed infrequent breaks in the outer longitudinal tract, while occasional thinning of these tracks were observed with BP102 (Figures 3B, G; Table 1). We could not address whether protein was reduced in spg^{242} animals as the stop codon at AA487 truncates the protein before the region against which the Spg antibody was produced. Thus, we chose to analyze spg^{242} over the deficiency line Df(3R)3450, which removes the *spg* locus [41]. In embryos of the genotype $spg^{242}/Df(3R)3450$, we observed a similar percentage of gaps in the outer longtudinal fascicles to that of spg^{242}/ spg^{242} (Table 1). Furthermore, the frequency of outgrowth defects observed in $spg^{805}/Df(3R)3450$ and spg^{242}/ spg^{805} alleleic combinations were consistent (Table 1, Supp. Figure 1). To see if we could observe increased defects via neuronal-specific knockdown of Spg, we expressed *UAS-spg RNAi* using the pan-neuronal driver *C155-GAL4*. In addition to increased axon outgrowth defects (Table 1), we observed occasional bifurcated bundles, indicative of fasisculation or abnormal fusion defects (Supp. Figure 1E). The localization of *spg* expression in the developing nerve cord and Spg-ELMO complex based upon mass spectrometry results led us to examine the role of *elmo* genetically in development of the CNS. As predicted based upon the maternal contribution of ELMO mRNA and

protein, embryos homozygous mutant for *elmo*^{19F3}exhibited minor defects in axonal patterning. FasII labeling revealed a nearly wild-type pattern of all longitudinal fascicles, while occasional thinning of these tracks and increased length of adjacent segments were observed with BP102 (Figures 3C, H; Table 1). As described in Geisbrecht et al., this allele contains a stop codon at amino acid 393 and appears to be null as removal of both the maternal and zygotic contribution of *elmo* by germline clone analysis (GLC) resulted in early embryonic lethality [21]. Consistent with this, FasII staining in embryos homozygous for the deletion allele *elmo*^{ko} [37] appeared normal (Table 2) and also resulted in early embryonic lethality when analyzed by GLC analysis. To reduce *elmo* function, yet allow animals to survive until the later stages of embryogensis when CNS development occurs, we used a hypomorphic *elmo* allele for GLC analysis [21]. In representative embryos maternally and zygotically mutant for *elmo*$^{PB(c06760)}$, a dramatic increase in axonal patterning defects were observed. In addition to an increased number of outer fascicle gaps, we saw aberrant midline crossing of longitudinal axons, and misrouting of outer longitudinal axons (Figures 3D, I; Table 2). This suggests that *elmo* functions in CNS development in addition to its role in myoblast fusion and border cell migration [21, 37].

If two genes act in the same pathway, transheterozygosity for the two genes of interest may result in a phenotype stronger than the single mutants alone. This type of experiment is complicated in the case of *elmo* and *spg,* which are both contributed maternally. To examine if loss-of-function phenotypes could be exacerbated by removal of genes that function in the same pathway, zygotic embryos of the genotype *elmo*^{19F3}*/elmo*^{19F3}*;spg*^{242}*/spg*^{242} were analyzed. Compared to *elmo/elmo* (0.0%; n=133) or

spg/spg (10.0%; n=100) single mutants, a consistent increase in longitudinal axon defects were observed in the double mutants (37.7%; n=106; Table 2). In addition, we observed an increase in axons that inappropriately cross the midline (Table 2). A representative example is shown in Figure 3E and quantified in Figure 3K. By BP102 staining, abnormalities in the spacing between adjacent segments was also enhanced (Figure 3J). There are two possibilities to explain this result: (1) the double mutant is phenotypically stronger than either single mutant as the residual maternal products are compromised; or (2) the stronger phenotypes observed in the double mutant combination are a result of two pathways being affected. The two possibilities are not mutually exclusive. We favor the first hypothesis as we know Elmo-Spg are found in a complex based upon our MS and IP results. Furthermore, we do not observe genetic interactions with other candidates that may function with *elmo*.

No muscle patterning defects are observed in mutants lacking Spg

Based upon the complementary expression patterns for *mbc* and *spg* in the somatic musculature and developing CNS, respectively, an attractive notion would be that ELMO binds to and functions with Mbc and Spg in a tissue-specific manner. To explore this, we examined phenotypes of single and/or double mutants in both muscle and nervous system development. Consistent with our above results that removal of zygotic *spg* exhibited almost wild-type axonal patterning, no myoblast fusion defects were observed in zygotic spg^{242}/spg^{242} mutant embryos (Figure 4A). In addition, we did not observe unfused myoblasts just under the somatic muscle layer (data not shown). In contrast to defects observed in the CNS in *elmo; spg* double mutants, analysis of the final

muscle pattern in these embryos appeared wild-type (Figure 4B). As previously reported, loss-of-function mutations in *mbc* resulted in strong myoblast fusion defects in the developing embryo [8, 20]. In homozygous embryos mutant for $mbc^{D11.2}$, the myoblasts were competent to migrate to the founder cells where fusion normally takes place, while fusion did not occur (Figure 4C). To examine if *spg* may be functioning redundantly with *mbc* in myoblast migration, the distribution of myoblasts was examined in $mbc^{D11.2}$, spg^{242}/ $mbc^{D11.2}$, spg^{242} double mutants. While the myoblasts fail to fuse as in *mbc* mutants, they were still capable of clustering around the founder cells, suggesting that myoblast migration was not affected (Figure 4D).

Both Spg and Mbc are required for axonal patterning

The experiments above indicate Spg is not required in embryonic muscle development. To further examine if Spg is the only DOCK family member required for axonal patterning, we examined the potential contribution of Mbc in the developing nervous system. Similar to defects already observed in *spg* mutants, embryos homozygous mutant for $mbc^{D11.2}$ exhibited breaks in the outer longitudinal fascicles (Figure 5A; Table 2). In addition, we observed collapse of axons onto the MP1 fascicle tracts (data not shown). This extends and supports observations by Nolan, et al., where it was determined that embryos transheterozygous for $mbc^{1.63}$/$mbc^{4.25}$ *exhibited ventral nerve cord defects upon examination with BP102* [25]. *Our analysis using BP102 phenocopies their results, where we observed thinning of the longitudinal axon tracts and abnormal spacing between segments (Figure 5C).* This suggests that low expression of

mbc, possibly undetected in the CNS due to high expression in the muscle, contributes to nervous system formation.

As Spg and Mbc are the two DOCK family members predicted to be specific for Rac and mutations in either one exhibit defects in the nervous system, we sought to examine if embryos mutant for both *mbc* and *spg* resulted in enhanced nervous system defects. We did not observe a significant increase in broken fascicles or the collapse of the outer longitudinal tracts in *mbc, spg* double mutants over *mbc* mutants alone (Figure 5B, Table 2). However, we did observe an increase in midline fascicle crossing in these double mutants (Figure 5B, arrows, Table 1). There was also an increase in abnormal positioning of the ventral nerve cord in *mbc, spg* double mutants, where 48.2% of mutant embryos (n=56) exhibited abnormal swerving of the nerve cord seen on the ventral side (Figure 5B, 5D) or abnormal bends in lateral views (Figure 5F compared to Figure 5E), which was rare in single mutants of *spg* (0.0%; n=23) or *mbc* mutants (0.8%; n=22). The above data suggests Mbc may be the primary DOCK family member in tissues like the muscle, while both Spg and Mbc may function in other tissues, such as CNS development and border cell migration.

Expression of N-cadherin is sufficient to recruit Spg to the membrane in S2 cells

Scanning through our list of potential MS candidates, N-cadherin (Ncad) emerged as a possible upstream receptor to mediate signaling via DOCK-ELMO complexes, albeit at low levels. Furthermore, Ncad is expressed in the embryonic fly nervous system and vertebrate MOCA/DOCK3 colocalizes with Ncad in regions of cell-cell contact in the nerve cell line PC12 [42, 43]. Thus, Ncad seemed a reasonable candidate to examine it's

involvement with DOCK-ELMO complexes in CNS development. To gain insight into a potential Ncad-Spg interaction, we examined the subcellular distribution of Spg and Ncad protein in *Drosophila* S2 cells. RT-PCR results show that *spg* is endogenously expressed in S2 cells (data not shown). Furthermore, staining with anti-Spg antibody reveals a cytoplasmic localization of the protein (Figure 6A). As S2 cells do not endogenously express *Ncad*, cells transfected with full-length Ncad were stained for Ncad and Spg protein. In transfected cells, Ncad was detected at the membrane and was capable of aggregating with other Ncad(+) cells (Figure 6B'), a hallmark of the homotypic cell adhesion properties of the Cadherin family of proteins [43]. The subcellular distribution of Spg was cytoplasmic in Ncad(-) cells (Figure 6A, 6A'', 6B, 6B''), but became membrane localized upon expression of Ncad (Figure 6A', 6A''). In Ncad(+) cells that formed clusters, Spg localization was enriched at the membrane between adjacent cells (Figure 6B', 6B''). To quantify these observations, we acquired confocal images of S2 cells both with and without Ncad expression. As shown in Fig. 6, we observed membrane-enriched Spg in 89.2% of cells (n=102) of Ncad (+) cells compared to 0.04% of S2 cells that do not express Ncad (n=210).

Genetic Analysis of Ncad-Spg mutants

Based upon the results that Spg is enriched at the membrane upon expression of Ncad in S2 cells, we wondered if removal of Ncad could increase the severity of spg^{242}/spg^{242} axonal phenotypes. As previously reported for other *Ncad* alleles, mutants for $Ncad^{405}/Ncad^{405}$*(Ncad)* alone show mild CNS defects (Figure 7A; Table 2) [43]. The Clandinin lab created mutants that remove both *Ncad* and the recently characterized *N*-

cadherin2 (Ncad, Ncad2 double mutant, hereafter called $Ncad^{D14}$) [44]. Thus, we examined $Ncad^{D14}$ mutants to determine if these proteins may function redundantly in CNS development. It appears the contribution of *Ncad2* is minor or negligible as our results do not show quantifiable differences between *Ncad* mutants alone or $Ncad^{D14}/Ncad^{D14}$ double mutants (Table 2). Removal of one copy of $Ncad^{D14}$ in a spg^{242}/spg^{242} homozygous mutant background increased the occurance of axon outgrowth defects over spg^{242} mutants alone (Table 2). To examine this further, we also quantitated embryos double mutant for both $Ncad^{D14}$ and spg^{242}. We observed a modest, although significant increase in axon outgrowth phenotypes over $Ncad^{D14}$ mutants alone (Figure 7C, Table 2). Consistent with this, $Ncad^{D14}$, $elmo^{19F3}$ double mutants exhibited a consistent enhancement of axonal breaks (Figure 7D, Table 2), although no increase in midline guidance errors. However, in both double mutant combinations, we also observed qualitatively different and/or stronger phenotypes than that observed in the single mutants alone. For example, we also observed a greater than additive increase in ectopic midline crossing in $Ncad^{D14}$;spg^{242} double mutants (23.0%) over $Ncad^{D14}$ (3.0%) or spg^{242} (0.0%) mutants alone. In $Ncad^{D14}$,$elmo^{19F3}$ double mutants, the embryos showed an increase in collapsed outer longitudinal axon tracts onto the MP1 fascicle (Figure 7D, asterisks), a phenotype not observed in $Ncad^{D14}$ or $elmo^{19F3}$ mutants alone. These data taken together suggest that the maternal load of *spg* or *elmo* may be masking phenotypes until the levels of an upstream component is compromised. An alternative explanation is that Ncad, Spg, or Elmo may also have functions independent of one another in CNS development. Although *mbc* is required for axon outgrowth (Figure 5A), we did not observe an increase

in axonal outgrowth or guidance defects upon removal of Ncad (Figure 7E), suggesting that Mbc may function independently.

A

	ELMO-HA					Untagged ELMO
Enzyme digestion[1]	Ti_1	Ti_2	Ti_3	Ti_4	Ti_5	Ti_1-3
ELMO (% coverage)[2]	43%[3]	68%	73%	50%	70%	2%
MBC (% coverage)[2]	6%	25%	36%	26%	29%	0%
CG31048 (% coverage)	2%	12%	20%	13%	12%	0%

[1]Ti=trypsin digest

[2]published in Geisbrecht, et al. 2008

[3]percentage of the protein sequence covered by detected peptides

B

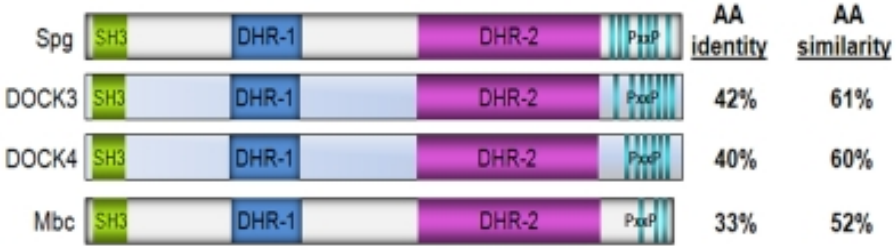

C

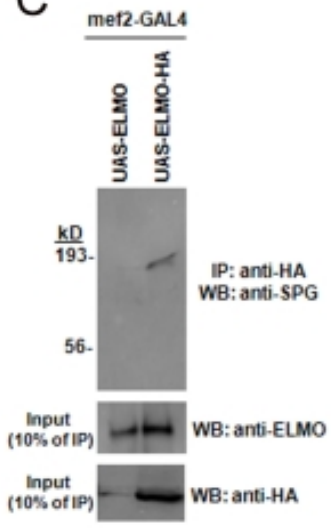

Figure 1: Identification of CG31048/Spg as an ELMO-binding Protein (A) Table showing peptide coverage of HA-tagged ELMO in 5 independent mass spectrometry experiments compared to 3 untagged ELMO control experiments. Aside from ELMO itself, the most abundant associated protein detected was Mbc, followed by CG31048. (B) Protein schematic of Spg and related proteins. Spg is the most similar to vertebrate DOCK3 and DOCK4. The most closely related fly protein is Mbc. SH3 (Src-homology domain-3); DHR-1 (DOCK Homology Region-1); DHR-2 (DOCK Homology Region-2); PxxP (Proline-rich region). (C) Both tagged and untagged ELMO are expressed under control of the muscle-specific *mef2-GAL4* driver. Embryonic lysates are immunoprecipitated with anti-HA and immunoblotted with antisera against Spg (top panel). Inputs show loading of total ELMO protein (middle panel) and HA-tagged protein (bottom panel).

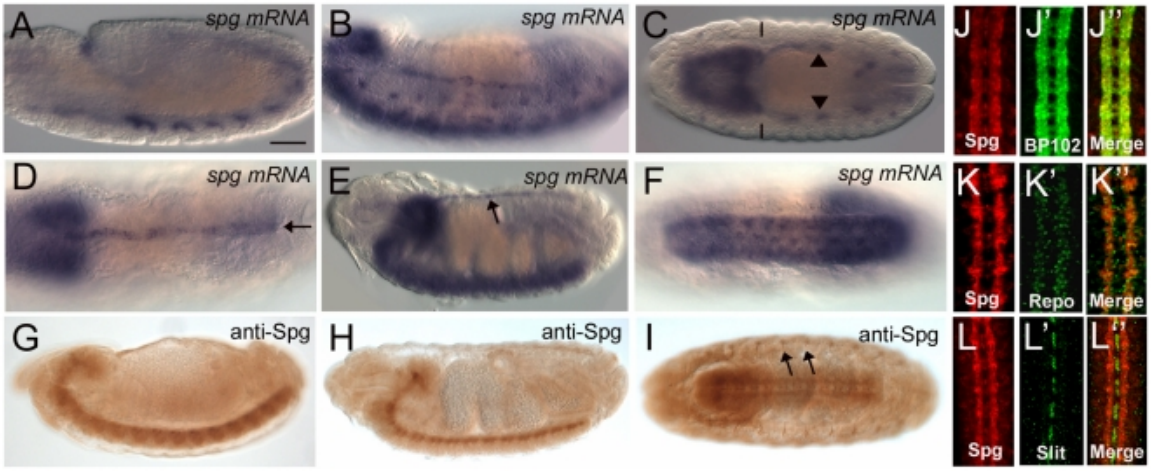

Figure 2: Spatial Expression of Spg in the Developing Embryo *In situ* hybridizations of wild-type embryos showing *spg mRNA* expression. (A–F) (A) Stage 11 embryo shows expression in the nervous system primordia. (B) Expression in the ventral nerve cord and sensory primordia at stage 13. (C, D) In dorsal views, *spg* is expressed in the brain and visceral mesoderm (arrowheads) at stage 13 (C) and brain and dorsal vessel at stage 16 (D, arrow). (E, F) At stage 16, expression is high in the ventral nerve cord in both lateral (E) and ventral (F) views. Arrow designates dorsal vessel expression (E). (G–I) Expression of Spg visualized by immunohistochemical staining. Spg is expressed is the ventral nerve cord in stage 13 (G) and stage 15 (H) embryos. Low expression is also detectable in the gut mesoderm (H). (I) A ventral view shows expression in the both the ventral nerve cord and peripheral neurons (arrows). (J-L″) Immunofluorescent confocal micrographs of Spg protein and neuronal markers. (J-J″) In stage 13 embryos, Spg expression overlaps with BP102 in both longitudinal and commissural axons. (K-K″) Spg is not expressed in repo (+) glial cells or ventral midline glial cells (L-L″). Anterior is left and dorsal is up in A, B, E, G, H. Scale bar=50 μm.

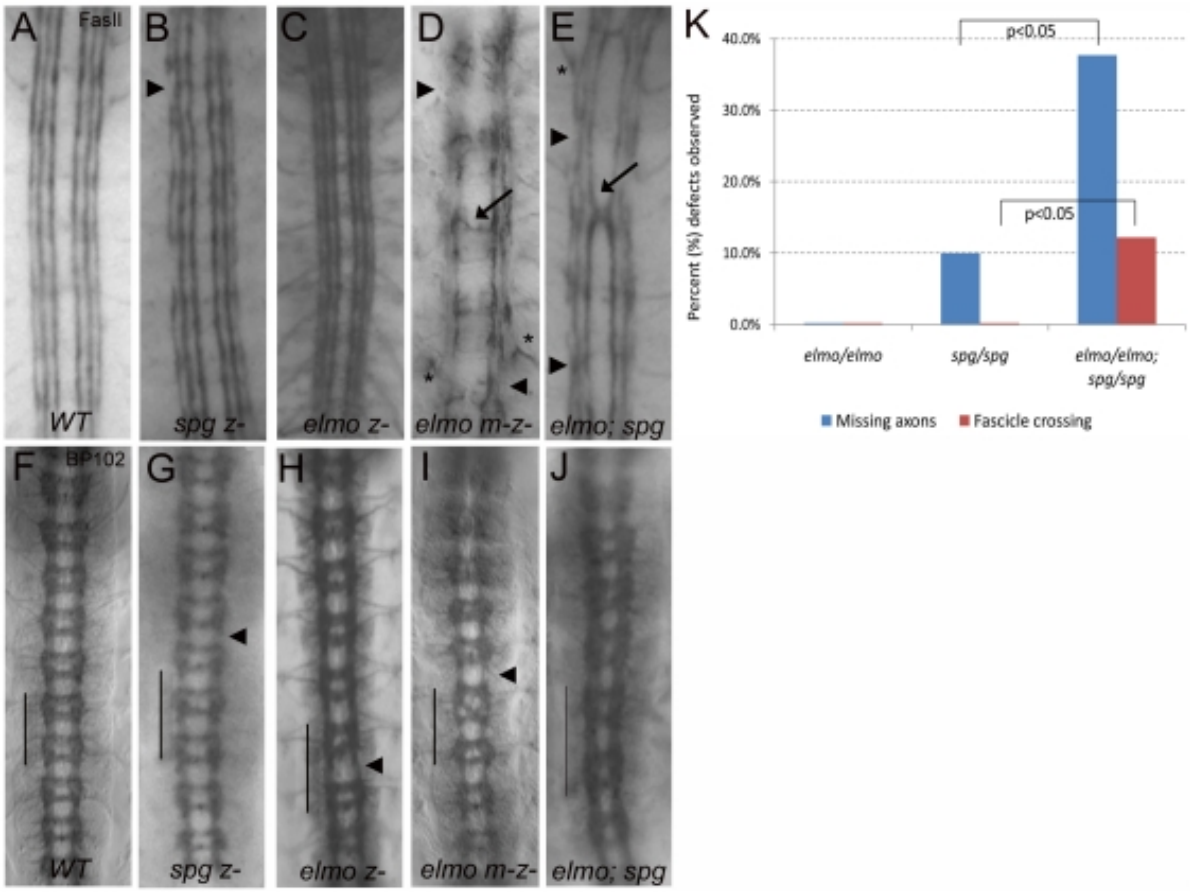

Figure 3: Embryos with Loss of Both Zygotic *elmo* and *spg* Exhibit Abnormal Axonal Patterns Late stage 16 or stage 17 embryos stained with anti-FasII to reveal subsets of longitudinal axons (A–E) and anti-BP102 to label all CNS axons (F–J). Anterior is up in all panels. (A, F) In WT embryos, FasII is expressed in 3 longitudinal bundles along each lateral side of the ventral nerve cord and BP102 labels both longitudinal and commissural axons on either side of the midline. (B, G) Removal of zygotic *spg* results in minor gaps in the outermost longitudinal fascicles (B, arrowhead) and a largely normal ladder-like pattern with occasional thinning of the longitudinal axons (G, arrowhead). (C, H) Embryos that lack zygotic *elmo* look similar to WT as visualized by anti-FasII (C) and

reveal minor thinning of longitudinal axons with anti-BP102 (H, arrowhead). (D, I) Removal of maternal and zygotic *elmo* visualized by FasII (D) reveal discontinuous bundles of lateral axon tracts (arrowheads) and aberrant midline crossing of fascicles (arrow). Misrouted 1D4-positive axons are also seen outside the normal longitudinal pathways (asterisk). (I) Thinner longitudinal axons (arrowhead) and abnormal commissural patterns are present with BP102 in *elmo m-z-* animals (I). (E) Analysis of embryos homozygous for both zygotic *elmo* and *spg* exhibit more severe axonal discontinuities and/or fusion to adjacent fascicles (arrowheads), in addition to inappropriate midline crossing (arrow). (J) These embryos also exhibit abnormal patterning of longitudinal and commissural axons (compare length of 2 consecutive segments denoted by line in J to F–I). (K) Graph depicting the percent of hemisegments that exhibit either gaps or missing axons and ectopic fascicle crossing in either *spg* or *elmo* mutants alone or *elmo*, *spg* double mutants. All embryos were stained with FasII for scoring (see table 1 for complete data set). Statistical significance was determined by student T-test.

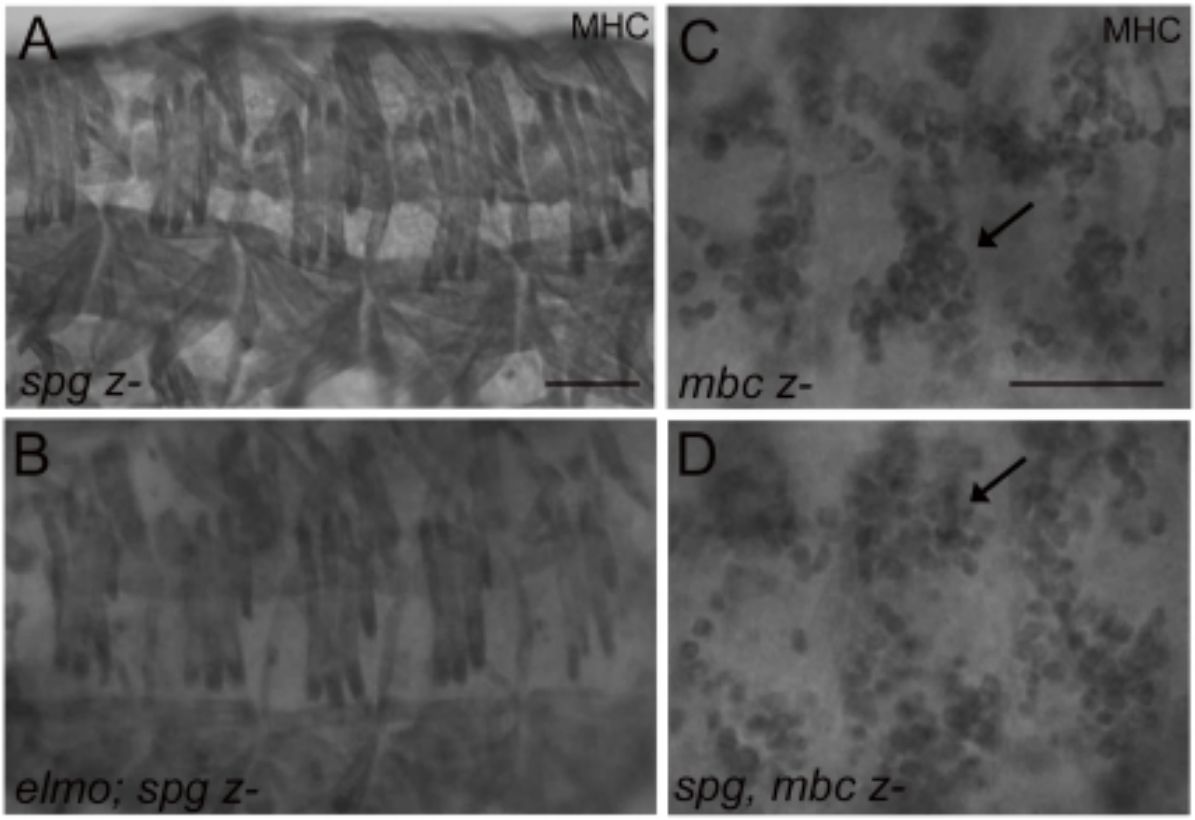

Figure 4: Loss of Zygotic *spg* is not Sufficient to Reveal Myoblast Fusion Defects (A–D) Lateral views of stage 16 embryos stained with anti-MHC to visualize the final muscle pattern. (A, B) A wild-type muscle pattern is seen in mutants that lack zygotic *spg* (A) and both zygotic *elmo* and *spg* (B). (C, D) Myoblasts fail to fuse but cluster around founder cells (arrows) in *mbc* mutants (C) and *spg*, *mbc* double mutants (D). Scale bar=10 μm.

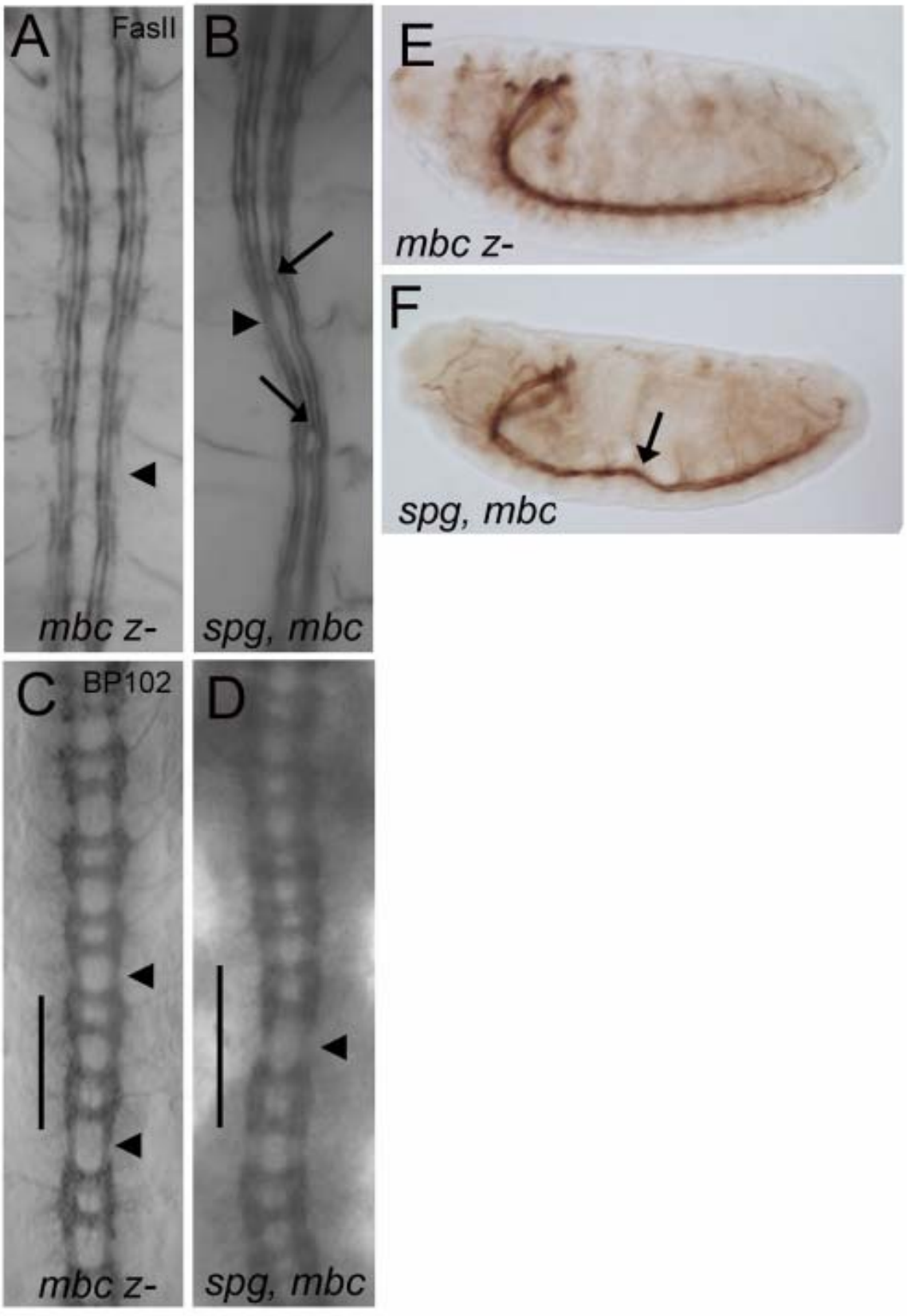
A
FasII
mbc z-
B
spg, mbc
E
mbc z-
F
spg, mbc
C
BP102
mbc z-
D
spg, mbc

Figure 5: CNS Defects are Enhanced in Embryos Missing Both *spg* and *mbc* Late stage 16 or stage 17 embryos stained with anti-FasII (A, B, E, F) and anti-BP102 to label all CNS axons (C, D). (A, C) *mbc* mutants have more discontinuities in the outermost fascicles (A, arrowhead) and thinner longitudinal axons (C, arrowheads). (B, D) Mutants missing both *spg* and *mbc* have an increase in (B) missing and collapsed longitudinal fascicles (arrowhead) and abnormal crossovers (arrows). BP102 staining (D) shows a severe thinning of axons (arrowhead) and abnormal spacing between segments (compare length of 2 consecutive segments denoted by line in panels C and D). (E, F) Lateral views of stage 16 embryos stained with anti-FasII show abnormal positioning of the ventral nerve cord in *spg*, *mbc* mutants (F, arrow) compared to *mbc* mutants alone (E). Anterior is up in panels A–D. Anterior is left and dorsal is up in panels E, F.

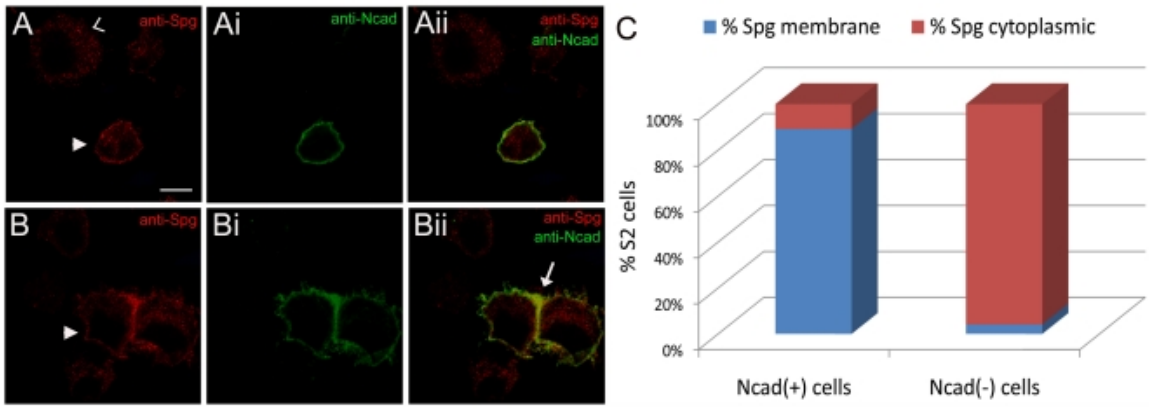

Figure 6: Expression of N-cadherin is Sufficient to Recruit Spg to the Membrane Late stage 16 or stage 17 embryos stained with anti-FasII (A, B, E, F) and anti-BP102 to label all CNS axons (C, D). (A, C) *mbc* mutants have more discontinuities in the outermost fascicles (A, arrowhead) and thinner longitudinal axons (C, arrowheads). (B, D) Mutants missing both *spg* and *mbc* have an increase in (B) missing and collapsed longitudinal fascicles (arrowhead) and abnormal crossovers (arrows). BP102 staining (D) shows a severe thinning of axons (arrowhead) and abnormal spacing between segments (compare length of 2 consecutive segments denoted by line in panels C and D). (E, F) Lateral views of stage 16 embryos stained with anti-FasII show abnormal positioning of the ventral nerve cord in *spg*, *mbc* mutants (F, arrow) compared to *mbc* mutants alone (E). Anterior is up in panels A–D. Anterior is left and dorsal is up in panels E, F.

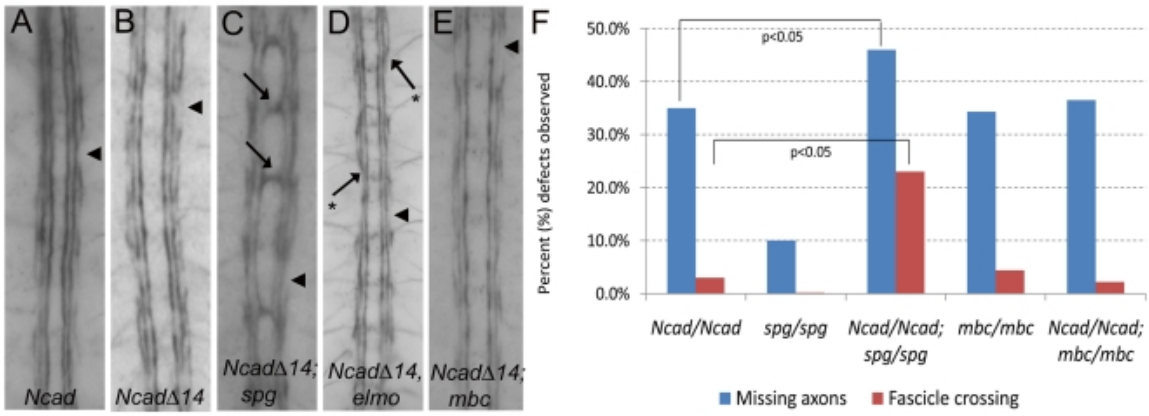

Figure 7: Genetic Interactions Between *Ncadherin*, *elmo*, *spg*, and *mbc* (A–E) Anti-FasII staining to visualize longitudinal axons. (A, B) Removal of zygotic *Ncad* (A) or both N-cadherin genes (*NcadΔ14*) (B) exhibit mild axonal break defects (arrowheads). (C) A significant increase in both fascicle axonal breaks (arrowhead) and ectopic midline crossing (arrows) are observed in *NcadΔ14*; *spg* double mutants. (D) Removal of both *NcadΔ14* and *elmo* function results in an increase in axonal patterning defects, including a collapse of the outer fascicle tract onto the MP1 fascicle (asterisk and arrow) and an increase in axonal gaps (arrowhead). (E) *NcadΔ14*; *mbc* double mutants exhibit many breaks in the outer longitudinal fascicles (arrowhead), similar to that of *NcadΔ14* or *mbc* alone. (F) Graph showing the percent of hemisegments that exhibit missing axons or ectopic fascicle crossing in *NcadΔ14*, *spg*, or *mbc* single and double mutants. A statistically significant difference (using student t-test) is observed in *NcadΔ14*; *spg* double mutants versus the *NcadΔ14* or *spg* single mutants alone. However, analysis of double mutants of *NcadΔ14*; *mbc* do not show a significant increase in axonal defects over the single mutants alone.

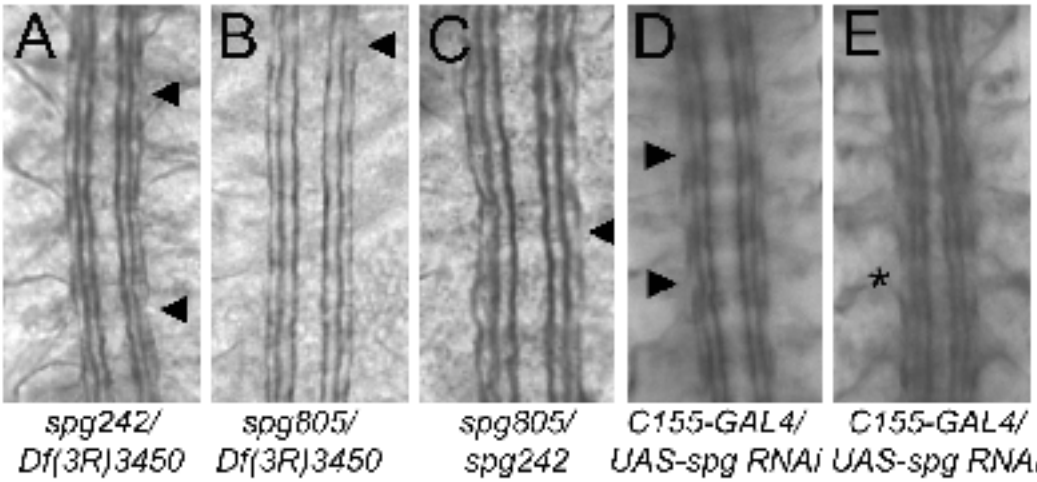

Figure 8: Loss of Spg results in mild CNS defects (A–E) Stage 16 embryos stained with FasII. (A, B) Both *spg242* (A) and *spg805* (B) over a deficiency that removes the *spg* locus result in mild gaps in the outer longitudinal fascicles (arrowheads). (C) The same phenotype are observed in animals trans-heterozygous for *spg242* and *spg805*. (D, E) Knockdown of Spg by RNAi resulted in similar axonal outgrowth phenotypes (D) and bifurcated axons (asterisk in E).

Table 1: Genetic Interactions between *elmo, spg, mbc,* and *N-cad*

Genotype	Missing Axons[a]	Fascicle Crossing[b]	% Segments Abnormal[d]	Segments Scored (n)	% Embryos severe to quantitate
y, w	0 (0.0%)	0 (0.0%)	0.0%	101	0.0% (n=15)
$elmo^{KO}/elmo^{KO}$	1 (0.8%)	0 (0.0%)	0.8 %	133	0.0% (n=16)
$elmo^{PB}$ *m-z-*	35 (44.8%)	5 (6.4%)	72.0%	79	0.0% (n=17)
spg^{242}/spg^{242}	10 (10.0%)	0 (0.0%)	10.0 %	100	0.0% (n=23)
$elmo^{KO}/elmo^{KO}$; spg^{242}/spg^{242}	40 (37.7%)**	13 (12.2%)**	50.0 %	106	0.0% (n=21)
$mbc^{D11.2}/mbc^{D11.2}$	23 (34.3%)	3 (4.4%)	38.8 %	69	0.0% (n=21)
spg^{242}, $mbc^{D11.2}/spg^{242}$, $mbc^{D11.2}$	97 (39.7%)	23 (9.4%)	49.1 %	244	11.3% (n=63)
$Ncad1^{405}/Ncad1^{405}$	24 (23.0%)	3 (2.8%)	25.9%	104	0.0% (n=17)
$Ncad^{1.14}/Ncad^{1.14}$	81 (35.0%)	7 (3.0%)	38.0%	231	0.0% (n=43)
$Ncad^{1.14}/Ncad^{1.14}$, $elmo^{19F3}/elmo^{19F3}$	133 (56.1%)**	10 (4.2%)	60.3%	237	4.7% (n=63)
$Ncad^{1.14}/Ncad^{1.14}$; spg^{242}/spg^{242}	97 (46.0%)**	48 (23.0%)**	69.7 %	208	7.4% (n=27)
$Ncad^{1.14}/Ncad^{1.14}$; $mbc^{D11.2}/mbc^{D11.2}$	115 (36.5%)	7 (2.2%)	38.7 %	315	6.0% (n=19)

Stage 16-17 embryos stained with anti-FasII were scored.
[a]Longitudinal axon tracts missing from either or both sides of nerve cord/segment.
[b]Normal fascicle(s) ectopically crossing the midline
[c]% segments abnormal includes all defects observed in a and b
m-z- designates removal of maternal and zygotic contribution
**indicates $p<0.05$ using student T-test compared to single mutants alone

CHAPTER 3

DIFFERENTIAL ROLES OF THE UNCONVENTIONAL DOCK FAMILY MEMBERS MYOBLAST CITY AND SPONGE IN *DROSOPHILA* DEVELOPMENT

Mbc and Spg do not function redundantly in somatic muscle development

Rho GTPases are enzymes that bind and hydrolyze GTP, allowing for physical interactions with downstream proteins to activate pathways involved in cell morphogenesis, including cell migration, cell adhesion, and phagocytosis [1, 2]. Normal development and tissue homeostasis require proper regulation of the GTP hydrolysis cycle to tightly control cytoskeletal cell shape changes and cell-cell adhesion events [3]. Inappropriate control of cell morphogenesis can manifest in abnormal cellular behaviors. For example, cancer cells may detach from their original location, undergo cytoskeletal rearrangement, and alter membrane adhesion dynamics to migrate through complex extracellular environments in tumor metastasis. Many of the same molecules are essential for cell morphogenic events in both normal and abnormal cells [4]. Thus, determining the normal function of proteins that control GTPases allows us to extrapolate how abnormal misregulation of cellular events result in genetic birth defects or disease progression in different biological contexts.

The Rho GTPases are key regulators in cell morphogenesis, cycling between an "off" and an "on" state [45, 46]. GTPase Activating Proteins (GAPs) facilitate the exchange of GTP for GDP to inactivate GTPases. Counteracting this, GEFs assist in the exchange of GDP for GTP, which activates GTPases for the binding to downstream effector proteins. This GDP exchange of Rho GTPases is facilitated by two types of GEFs; the Dbl family and the Dock family. Proteins of the Dbl family contain conserved tandem

Dbl homology (DH) and Pleckstrin homology (PH) sequences [1, 2]. Functionally, the DH domain catalyzes GEF activity, while the PH domain allows for interactions with other proteins to control sub-cellular localization [46, 47]. The 'atypical' Dock GEFs lack the canonical DH domain, but utilize an internal Dock homology region 2 (DHR2) for GTPase binding and exchange activity. Dock GEFs also contain a separate SH3 domain that interacts with the adaptor protein ELMO for the regulation of Dock protein localization and GTPase activation [1, 2]. The bipartite Dock-ELMO complex is required for optimal *in vivo* GEF activation of Rac [1, 48]. The current model suggests that ELMO and Dock exist in an autoinhibitory state in the cytoplasm and upon stimulation by external cues, this inhibition is relieved for ELMO-Dock complex membrane recruitment and interaction with downstream GTPase targets [1].

There are 11 Dock proteins in mammals that are subdivided into four categories: Dock A-D. To date, Dock-A, -B, and -C family members can all activate the Rho GTPase Rac, while Dock-C and –D proteins also show specificity for Cdc42 [1, 2]. Expanding the repertoire of GTPase targets, the Dock-B subgroup member Dock4 has also been shown to activate the Ras-like small GTPase Rap1 [26-28]. The Dock-A family member, Dock1 (Dock180), is required for vertebrate neuronal pathfinding, endothelial cell migration, and functions in concert with a second Dock-A member, Dock5, to control myoblast fusion in vertebrate muscle development [49-51].

Less is known about the developmental roles of the mammalian DockB family. Two of the subfamily members, Dock3 (also called Modifier of cell adhesion, or MOCA) and Dock4, are expressed in nervous system tissue, and Dock4 expression is also detected in smooth muscle cells [29-31]. Both Dock3 and Dock 4 are implicated in actin

reorganization through the activation of Rac in neurite outgrowth and dendritic spine morphology, respectively [52]; HIRAMOTO *et al.* 2006; UEDA *et al.* 2013). Notably, *Dock3*$^{-/-}$ mice exhibit neuronal degeneration [53]. The association of Dock 3 or Dock 4 in neurological disorders, including Alzheimer's disease, schizophrenia, and autism spectrum disorders, suggest a broader role in neuroprotection [2, 30, 32, 54]. An additional role for Dock protein was demonstrated in tumorigenesis. A representational difference analysis (RDA) screen using mice-derived tumors identified a single Dock4 point mutation in two different cancer cell lines [26]. This same study showed Dock4-mediated Rap activation was required for cells to maintain their cell-cell adhesion junctions. Clearly, these studies show the importance of Dock proteins in disease progression. However, overlapping expression patterns and functional redundancy in vertebrate models can be complicated. Fortunately, the less complex fly model provides an excellent system to examine the cellular roles of Dock protein function.

Redundancy is simplified in flies with only one Dock homolog per subfamily. In *Drosophila*, the Dock-A counterpart, Myoblast City (Mbc), is required for Rac-mediated processes, such as myoblast fusion and border cell migration that require modulation of the actin cytoskeleton [55, 56]. Mbc also functions redundantly with the Dock-B homolog, Sponge (Spg), in border cell migration [33]. However, it is unclear if these two GEFs function redundantly in other developmental processes in *Drosophila* where *spg* and *mbc* exhibit either overlapping or exclusive mRNA expression patterns. For example, *mbc* transcript is enriched in the somatic muscle and *mbc* mutants show myoblast fusion defects [21, 55, 57]. *Spg mRNA* is not detectable in the developing musculature and thus far no muscle phenotypes have been observed. In contrast, *spg,* but not *mbc* transcript is

high in the developing CNS, but mutations in either gene result in axon guidance or outgrowth phenotypes. While both *spg* and *mbc* are essential for CNS development, *spg* exhibits a genetic interaction with the cell adhesion molecule *N-cadherin*, while *mbc* does not [29]. These data, taken together, suggest that Dock family proteins may exhibit differential roles in development. One prediction of these different roles may be activation of different downstream GTPases. This is supported by a recent report where Spg is required for Rap-mediated photoreceptor differentiation in the *Drosophila* eye [28].

Herein, we use the genetically tractable model organism *Drosophila melanogaster* to determine if Mbc and Spg function redundantly in tissues other than border cell migration and to establish if these Dock proteins target the same or different GTPases in the dorsal vessel, a tissue where both transcripts are expressed [29]. Using genetic interaction analyses, RNAi knockdown, and rescue experiments with the GAL4/UAS system, we have established that Mbc and Spg have differential functions in the development of the somatic muscle and dv. In addition, we show that the downstream GTPases of these GEFs are different in dv development. This is one of the first *in vivo* examples of these two related proteins having distinct targets in development.

Myoblast fusion defects are well described in *Drosophila* somatic muscle development, a process analogous to skeletal muscle development in mammals and requires the regulated control of cell morphogenic events [58]. At stage 13 in embryogenesis, specialized muscle cells termed founder cells are present at sites where somatic muscles will eventually form. Fusion competent myoblasts migrate to these founder cells and undergo repeated rounds of myoblast fusion events to form multinucleated muscle fibers (Fig. 1A,B). Consistent with published literature [55, 59],

mutations in the gene that encodes for the *Drosophila* DockA homolog *mbc,* resulted in myoblasts that were capable of migrating to the founder cells, but failed to undergo fusion (Fig. 1C; arrowhead). Our earlier studies showed that removal of *spg* in an $mbc^{-/-}$ mutant background does not alter the ability of myoblasts to migrate to or fuse with founder cells [29]. These data strongly suggest that Mbc and Spg do not perform the same roles in the migration or fusion of myoblasts during somatic muscle development.

A limiting factor in the analysis of $mbc^{-/-}$ $spg^{-/-}$ double mutants is the presence of maternal *spg* transcript [29, 35], possibly masking our ability to observe an enhancement of *mbc* phenotypes. To circumvent the issue of *spg* maternal contribution and address whether Dock proteins exhibit functional redundancy using a different assay, we tested whether Spg could compensate for the $mbc^{-/-}$ myoblast fusion phenotype**.** Expression of *UAS-mbc* under control of the mesodermal-specific GAL4 driver, *twist (twi)*, fully rescued the muscle pattern to WT in over 80% of the embryos in an $mbc^{-/-}$ mutant background (Fig. 1D,F). Ectopic expression of full-length *spg* (*UAS-spgFL)* did not rescue *mbc*-induced myoblast fusion defects to the same extent as expression of *mbc* (Fig. 1E,F). We occasionally observed a few fully formed myotubes in this genotype (14.3%), suggesting that a small portion of Spg protein could compensate for the loss of Mbc. Overall, we conclude that Mbc and Spg do not have equivalent roles in somatic muscle development.

The Mbc-Elmo complex functions upstream of Rac1 in myoblast fusion

Previous experiments to rescue myoblast fusion defects in *mbc* mutants using the constitutively active form of Rac ($UAS\text{-}Rac1^{V12}$) have been difficult to interpret due to the

drastic phenotypes of activated Rac on its own (Fig. 2E), and possibly additional functions of Mbc that cannot solely be rescued by a single downstream molecule [60]. Thus, we chose a different genetic approach to examine if the Mbc-ELMO complex acts upstream of Rac in myoblast fusion. We used the *mef2* promoter to express either *UAS-mbc* or *UAS-elmo* in the developing musculature. Either the *mef2-GAL4* insertion alone (Fig. 2A,B) or overexpression of *mbc* (Fig. 2C) or *elmo* (Fig. 2D) did not induce myoblast fusion defects. However, simultaneous overexpression of *mbc* and *elmo* triggered myoblast fusion defects (Fig. 2G) similar to, but less severe, than ectopic expression of the neuronal DH-containing Rac1 GEF *trio* (Fig. 2F). We next found that we could suppress fusion defects due to overexpression of an Mbc-ELMO GEF complex upon removal of a single copy of the downstream GTPases *Rac1* and *Rac2* (Fig. 2H), both of which are required for myoblast fusion [23]. These data demonstrate that the Mbc-ELMO complex function upstream of the Rac GTPase to regulate myoblast fusion in the developing *Drosophila* embryo.

Spg and Mbc are required for dv development

We previously showed that *mbc* and *spg mRNA* are both expressed in the developing dv [29], and we decided to use this tissue to further assay the cellular roles of Dock proteins. Formation of the *Drosophila* dv, or heart tube, begins around st. 13 of embryonic development after heart cell specification has delineated two rows of 52 precursor cells, or cardioblasts, on the dorsal side of the embryo (Fig. 3A,B). The cardioblast rows are physically linked to the epidermis and migrate towards the dorsal midline as dorsal closure proceeds. By st. 17 the cardioblast cells are paired up at the

dorsal midline with a distinct posterior heart and anterior aorta region [61] (Fig. 3A',B'). This alignment of cells provides a simple assay to analyze gene functions in early and late stages of dv morphogenesis.

Previous analysis of *spg*$^{-/-}$ mutants, which contained maternally contributed *spg,* showed only mild defects in CNS development [29]. Thus we sought a different approach to further knockdown Spg levels using an RNAi strategy in a *spg*$^{-/-}$ mutant background. Expression of *UAS-spgRNAi*^{353} in the developing musculature (*24B-GAL4*) in zygotic *spg*$^{-/-}$ mutants resulted in weak cardioblast clustering defects in both early (Fig. 3C) and late stages (Fig. 3C') of dv development. Expression of a new embryonic lethal RNAi line (*UAS-spgIR*^{13}) [28] with the mesodermal-specific GAL4 drivers, *twi* (Fig. 3D,D') or *24B* (Fig. 3E,E'), revealed enhanced clustering of the cardioblasts that persisted from st. 13 (Fig. 3I and Table 1A) until st. 17 (Table 2A). Importantly, these clustering defects were severe, with some clusters containing four or more cells. Analysis of single sections from multiple Z-stacks showed that many clusters resulted from cells on top of other cardioblasts. To confirm this observation, we imaged a lateral view of the dv in st. 13 embryos. The cardioblasts in WT embryos formed a single-celled row (Fig. 3F), whereas these same cells appeared clustering on top of one another in *twi-GAL4::UAS-spgIR*^{13} embryos (Fig. 3G). This data suggests defects in the ability of the cardioblast rows to maintain their initial contralateral alignment at the beginning of dv development. To our knowledge, this is the first report of a multilayered cell clustering phenotype in a *Drosophila* dv mutant.

The above data clearly show a requirement for Spg in patterning of the dv. We next decided to test if *mbc*$^{-/-}$ mutant embryos also exhibited defects in heart tube

morphogenesis. Cardioblast clustering defects were apparent in *mbc*$^{-/-}$ mutants at st. 13 (Fig. 4A; arrowhead). However, the number of cells in each cluster was consistently less than those observed in *spg*$^{-/-}$ mutants (Tables 1,2) and the clusters were never multilayered (compare arrowhead in Fig. 3G to Fig. 3H). Furthermore, the clustering defects observed in early *mbc*$^{-/-}$ mutants were often adjacent to breaks in the lateral rows of cardioblasts (Fig. 4A; arrow), indicating that the cluster may be a result of this break. Clusters seen in regions of the cardioblast row that were not next to a break normally consisted of only two cells compared to the complex clustering in *spg*$^{-/-}$ mutant animals that contained at least four cells.

Cardioblast clusters observed in early *mbc*$^{-/-}$ mutant embryos persisted until st. 17 (Fig. 4A'; arrowhead). We also observed regions along the length of the dv that consisted of unpaired, or rows of single cells (Fig. 4A'; brackets). It is unclear if this phenotype is a manifestation of the gaps seen in early *mbc*$^{-/-}$ mutants, a loss of cell number during the migration process, or a twist in the vessel where the cells end up underneath their potential paired cardioblasts. Quantification of cardioblasts showed a loss of about 10 heart cells in *mbc*$^{-/-}$ mutants from st. 13 to st. 17 (Table 1B,2B). This analysis was performed by counting individual cardioblasts in single sections of confocal z-stacks, reducing the possibility of missing cells that could be underneath other cardioblasts. This single cell phenotype has been reported in another dv mutant, *laminin-A*, and is thought to result from the inability of the dv to maintain its position within the embryo, resulting in twists and breaks in the cardioblast rows [62]. These data, taken together, show that while loss of either GEF results in cardioblast clustering, the clustering in *spg* mutants is

more severe than *mbc* mutants. Moreover, *mbc* mutants are characterized by a loss of cardioblast cells and lateral gaps within a contralateral row of cells.

Spg is not capable of rescuing defects resulting from mbc removal in the dv

To verify and extend our observations that Mbc and Spg play independent roles in dv morphogenesis, we utilized the GAL4/UAS system to perform rescue experiments specifically in the dv. As expected, the reintroduction of *UAS-mbc* was sufficient to ameliorate the loss of cardioblast cell numbers, rows of single cells, and clustering defects present in *mbc* mutants (Fig. 4B,B,E,F and Table 1B,2B). In contrast, expression of *UAS-spg* did not suppress any of these dv phenotypes to the same degree (Fig. 4C, C', E, F and Table 1B,2B). Note that while we could not directly assay the extent of somatic myoblast fusion with the Mef2 muscle nuclei marker used in these experiments, we noticed a change in the organization of the dorsal muscle nuclei. Consistent with the well-documented myoblast fusion defects in $mbc^{-/-}$ mutants (Fig. 4A'; carets), we saw a general disorganization of the somatic nuclei in this genotype that was restored upon expression of *UAS-mbc* (Fig. 4B'; asterisks). This rescue did not occur upon expression of *UAS-spg* (Fig. 4C'; caret), which is consistent with our data in Fig. 1 showing that Spg does not rescue *mbc*-induced myoblast fusion defects.

The overall primary amino acid sequence between Mbc and Spg (33% identity/52% similarity) is the most divergent in the C-terminal proline-rich region, where the identity decreases to 16% and similarity to 21% [29]. This feature prompted us to create a mutant form of Spg that lacked this proline rich region; called *UAS-spgΔPxxP*. Expression of *UAS-spgΔPxxP* in $mbc^{-/-}$ mutants produced an intermediate rescue,

suggesting that in addition to the DHR2 domain, the C-terminal rich domain may play a role in dv development (Fig. 4D,D,E,F and Table 1B, 2B).

GTPase activation of both Rac1 and Rap1 is required for proper dv development

To address our central question of whether Dock family members act upstream of different GTPase targets *in vivo*, we first examined if disruption of Rac or Rap1 affected dv morphogenesis. Zygotic removal of both *Rac1* and *Rac2* induced small cell clusters and lateral gaps that were prevalent at st. 13 (Fig. 5A,G and Table 1C) and persisted in embryos analyzed at st. 17 (Fig. 5A',H and Table 1C). Since both *Rac1* and *Rac2* are maternally contributed gene products [23], we expressed a dominant negative form of *Rac1 (UAS-Rac^{N17})* under control of the *twi* promoter to observe effects upon loss of Rac activity. In addition to an increased penetrance of clustering defects, we also observed partial rows of single cells and a loss of cardioblast number not observed in *Rac1Rac2$^{-/-}$* mutants alone (Fig. 5B, B' G, H and Table 1C, 2C). These combined phenotypes were similar to dv defects in single *mbc$^{-/-}$* mutants and in embryos that were doubly mutant for both *mbc* and *elmo (*Fig. 5C, C' and Table 1C, 2C).

We observed a similar trend in the degree of penetrance observed upon loss of Rap1, where the weak phenotypes observed in zygotic *Rap1$^{-/-}$* mutants were increased upon expression of dominant-negative Rap1 (*UAS-Rap1^{N17}*). *Rap1$^{-/-}$* mutants showed mild clustering defects in both early (Fig. 5D,G and Table 1C) and late dv development (Fig. 5D',H and Table 2C). In addition to an increase in the number of clusters per embryo, gaps in the contralateral rows, were also present upon expression of *UAS-Rap1^{N17}* in the dv (Fig. 5 E, E' and Table 1C, 2C). Note that loss of Rap activity did not

alter cardioblast number (Fig. 3H and Table 1C). Removal of both *spg* and *elmo* resulted in severe cardioblast clustering, reminiscent of that seen in *UAS-spgIR*^{13} knockdown (Fig 5F,F' and Table 1C, 2C). As illustrated in Fig. 5, the cardioblasts in some st. 13 embryos exhibited a "star" phenotype, suggesting that the dv is either being pulled away from or restrained from migrating to the central midline. Importantly, *elmo*$^{-/-}$*; spg*$^{-/-}$ double mutant animals were unhealthy and even heterozygotes had a hard time surviving under normal laboratory conditions. Taken together, these data suggest that both Rac and Rap1 are required for dv development.

Mbc exhibits specificity for Rac in dv morphogenesis

We next tested if Mbc acts upstream of Rac1 in the developing heart tube as it does in somatic muscle development. Expression of *UAS-Rac1*^{V12} under control of the *twi* promoter resulted in the same phenotypes, but with increased penetrance, as those observed in *mbc*$^{-/-}$ mutants, including cell clustering (small arrows), gaps in the cardioblast rows (long arrows) and regions of single cells (Fig. 6A,A'; bracket). Expression of *UAS-Rac1*^{V12} in an *mbc*$^{-/-}$ mutant ameliorated these phenotypes nearly to WT (Fig. 6B, B', D, E). Notably the decrease in cardioblast number was also rescued upon reintroduction of *UAS-Rac*^{V12} (Table 1D, 2D), a suppression that was not observed upon overexpression of *UAS-Rap1*^{V12} (Fig. 6C,C',D,E and Table 1D, 2D), strongly suggesting that Mbc acts upstream of Rac and not Rap1 in this tissue.

Spg and Rap1 likely function together in dv development

Since the dv defects in *mbc*$^{-/-}$ mutant embryos were partially suppressed upon the introduction of *UAS-Rac*^{V12}, we wondered if we could temper *spg*-induced phenotypes upon expression of *Rap1*^{V12}. As might be expected for either mis- or overexpression of a constitutively active form of any GTPase, patterning defects were present in the dv upon expression of *UAS-Rap1*^{V12}. Specifically, we observed an increased number of cardioblast clusters that persisted from early (Fig. 7A,F and Table 1E) to late (Fig. 7A' and Table 2E) stages along with some regions of single cells (Fig. 7A' and Table 2E). Expression of this constitutively active form of *Rap1* ameliorated the single cell clustering phenotypes associated with a reduction in *spg* levels using *UAS-spgIR*^{13} (Fig. 7B,B',F and Table 1E). Acquiring this stronger RNAi line allowed us to further investigate the involvement of Spg in CNS development [28, 29]. Using the neuronal *C155-GAL4* driver, RNAi depletion of *spg* resulted in increased penetrance of outgrowth defects (Fig. 7C; caret) and midline crossing errors (asterisk) compared to *spg*$^{-/-}$ mutants alone [29]. Expression of *UAS-Rap1*^{V12} in a *spg RNAi* background reduced the percentage of axon skipping and eliminated midline guidance defects (Fig. 7E,G). While this data suggests that Spg may function with Rap1, there are limitations in analyzing whether GTPase overexpression can suppress knockdown of a gene using RNAi techniques.

We next turned to genetic interaction analysis to further examine if *spg* and *Rap1* likely function in the same pathway in dv development. Removal of zygotic *Rap*$^{-/-}$ (Fig. 8A,A' and Table 1F,2F) or *spg*$^{-/-}$ (Fig. 8C, C' and Table 1F,2F) alone resulted in mild clustering defects. An enhancement in the number of cardioblast cells in each cluster was seen upon removal of either one copy of *spg* in *Rap1*$^{-/-}$ mutants (Fig. 8B,B',F and Table 1F,2F)

or a 50% reduction in *Rap1* gene dosage in a *spg*$^{-/-}$ mutant background (Fig. 8D,D',E and Table 1F,2F). Importantly, the cardioblast number did not change in our genetic interaction analysis between *spg* and *Rap1,* further supporting the idea that cardioblast number is mediated by the Mbc→Rac pathway. These data provide good evidence for Spg and Rap1 acting together in dv development.

Mbc and Spg are required for proper dv lumen formation

Cryosection and electron microscopy studies reveal that the dv is an excellent *in vivo* two-cell system to study cell morphogenesis [63, 64] Starting in st. 13 embryos, two contralateral rows of cardioblasts migrate towards the midline to form the first junctional adhesion domain by st. 15 (Fig. 9A'). The adhesion proteins β-catenin and E-cadherin accumulate at this initial adhesion site and trigger actin-mediated cell shape changes, in which the cardioblasts adopt a crescent-like shape to form a second, ventral adhesion site. Simultaneous with heart cell shape changes, cell-autonomous, repellant Slit/Robo signaling at the lumenal surface of the cardioblasts prevents ensures proper lumen formation [63-65].

We chose to test whether loss of *mbc* or *spg* resulted in aberrant cell shape changes during dv development and whether the adhesion between the cardioblasts was altered in these mutant backgrounds. Using transmission electron microscopy (TEM), analysis of cross-sections in WT st. 17 embryos showed two crescent-shaped cardioblasts with an internal lumen (Fig. 9 B'). Higher magnification revealed electron dense regions, indicative of adhesion complexes, at the junctional domains (Fig. 9 B''). In *mbc* mutants, the cardioblasts appeared rounded as if unable to change shape, and the lumen was either

absent or very small (Fig. 9C'). Dark electron dense regions were present in *mbc* mutants, suggesting that adhesion sites were present (Fig. 9C''). In contrast, the heart cells in *twiGAL4::UAS-spgIR*^{13} mutants showed an elongated shape (Fig. 9D') that was different from the crescent-like cells observed in WT embryos or the round cells in *mbc* mutants. This genotype also lacked a lumen and the electron dense regions seen in WT and *mbc* mutants (Fig. 9D''). These results show that both Mbc and Spg are required for lumen formation in dv morphogenesis, although they likely act through different signaling pathways as the morphology of the heart cells and presence of electron dense adhesion sites were not the same in the two mutant genotypes.

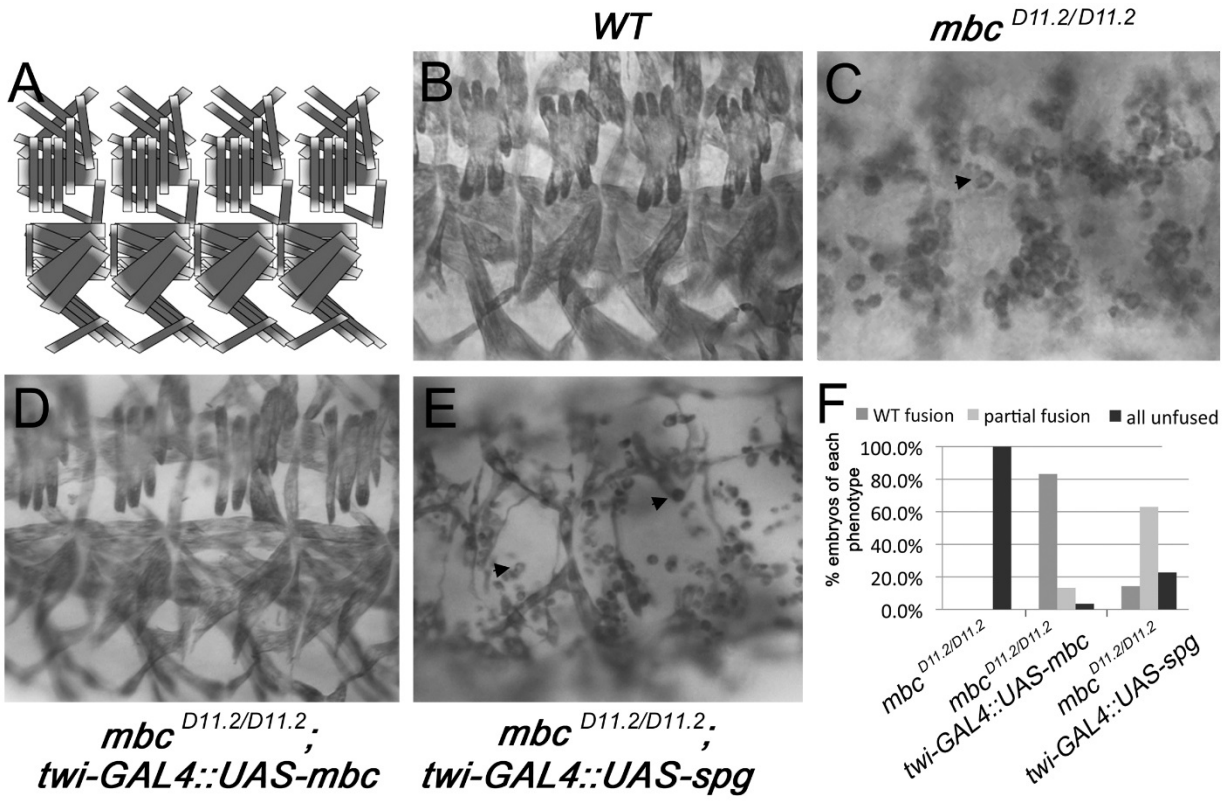

Figure 9: Spg cannot compensate for Mbc in myoblast fusion (A) Schematic representation of four hemisegments of the somatic musculature of a st. 16 embryo *Drosophila* embryo. (B-E) Late st. 16 embryos stained with α-MHC to visualize the somatic muscle. (B) WT embryos show organized repeating segments of somatic muscle. (C) Zygotic removal of *mbc* results in severe myoblast fusion defects (arrow). (D) Reintroduction of *mbc* specifically in the mesoderm using the *twi-GAL4* driver rescues the somatic muscle fusion defects. (E) However, expression of *spg* does not rescue the myoblast fusion defects to the extent as *mbc*. (F) Graph showing the extent of myoblast fusion rescue. Anterior is left and dorsal is up for all embryos. Scale bar: 20μm.

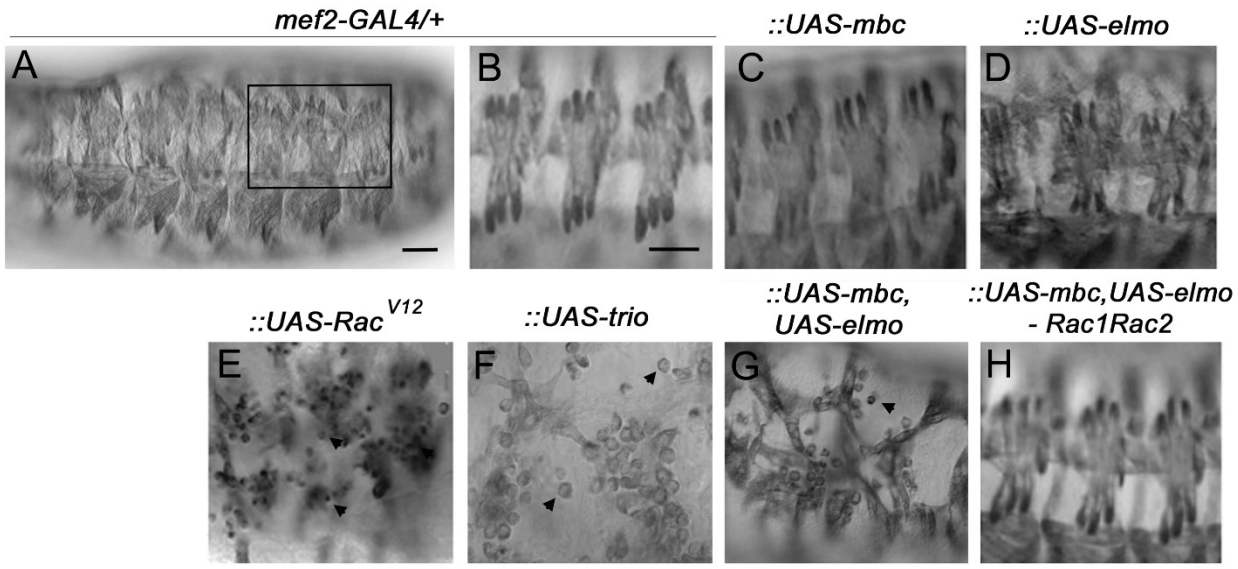

Figure 10: The Mbc-Elmo complex functions upstream of Rac1 in myoblast fusion (A-H) Late stage *Drosophila* embryos stained with α-MHC to visualize the somatic musculature. The muscle specific GAL4 driver, *mef2,* is used to drive the expression of indicated UAS constructs. (A, B) Whole mount view of the entire embryo (A) or a higher magnification photograph of three hemisegments (B) show normal repeating segments of organized muscles in embryos heterozygous for the *mef2-GAL4* driver. (C, D) Expression of *mbc* (C) or *elmo* (D) alone do not result in somatic muscle defects. (E-F) Expression of Rac^{V12} (E) or ectopic induction of the GEF, *trio*, show severe myoblast fusion defects (F). (G) Co-expression of *UAS-mbc* and *UAS-elmo* (G) induces somatic muscle fusion defects, which are suppressed upon removal of one copy of *Rac1* and *Rac2* (H). Anterior is left and dorsal is up for all embryos. Scale bar: 20μm.

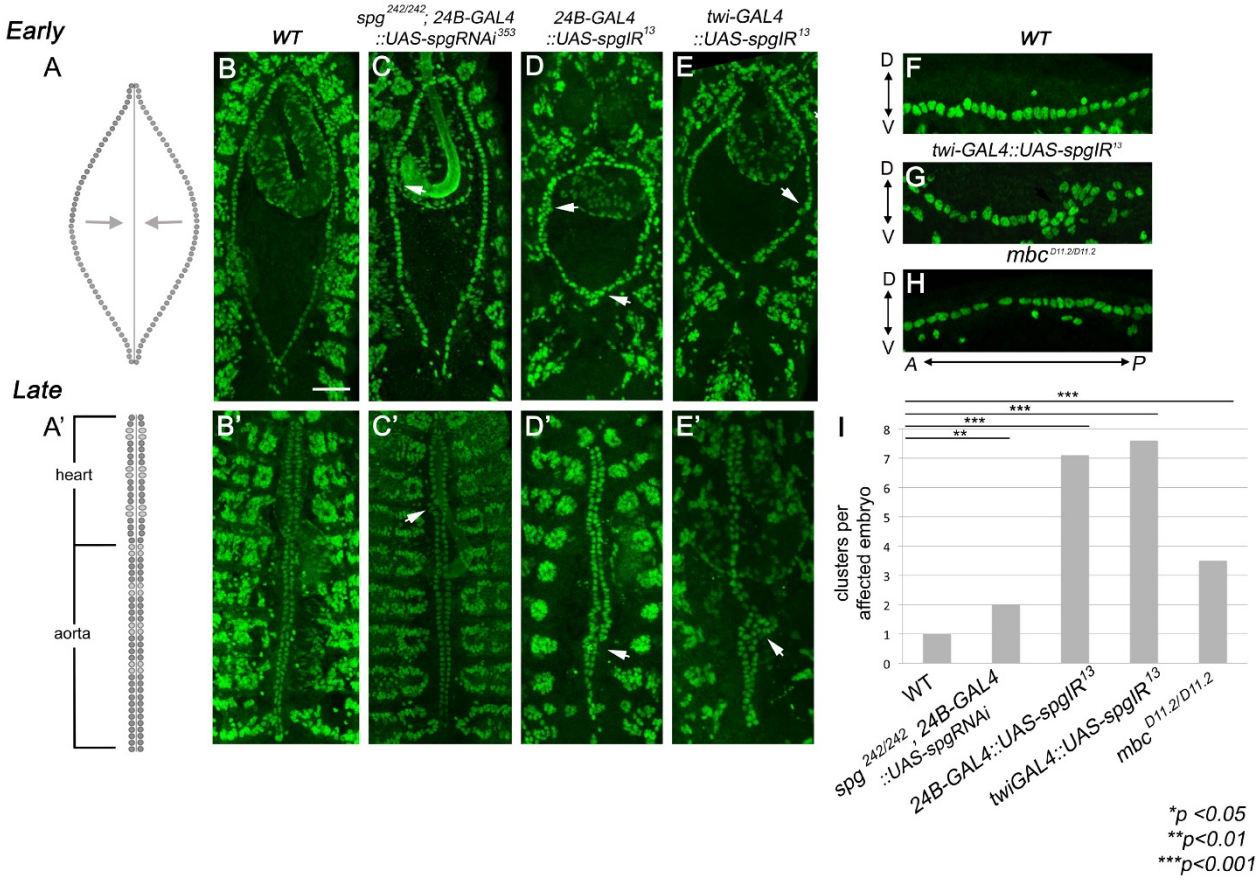

Figure 11: Spg is required for dorsal vessel patterning (A, A') Schematic representation of the cardioblasts. At the beginning of dv development, two rows of cardioblasts begin to migrate towards the dorsal midline (A, arrowheads). As dorsal closure proceeds, the opposing cardioblast rows eventually pair up at the midline where they form a distinctive posterior heart compartment and anterior aorta compartment (A'). (B-E') Dorsal views of cardioblast cells stained with the nuclear marker Mef2 in early (B-E) and late (B'-E') dv development. (B, B') WT embryos form two evenly spaced rows (B) that meet at the dorsal midline in pairs (B'). (C, C') Expression of *UAS-spgRNAi*^{353} with *24B-GAL4* in a *spg*$^{-/-}$ mutant background occasionally shows mild clustering defects (arrowheads). (D, D') Knockdown of *spg* with a different *UAS-spgIR*^{13} line under control of the *24B*

promoter results in severe clustering (arrowheads). (E, E') These severe clustering defects are also seen using the *twist* mesodermal driver (arrowheads). Note the severe clustering, sometimes containing more than 3 nuclei, seen in E-E' compared to the relatively mild clustering seen in C and C'. Scale bar: 50μm. (F-H) Lateral views of approximately four hemisegments stained with α-mef2 to visualize cardioblast cell nuclei. The heart cells in *WT* (F) and $mbc^{-/-}$ (H) embryos form a relatively straight line compared to multilayered clustering observed in $spg^{-/-}$ mutants (G). (I) Graph depicting the average clusters per st. 13 embryo in the indicated genotypes. *spg* mutants exhibit increased cardioblast clustering defects. Posterior is up for panels B-E'. Anterior is left for panels F-H. Scale bar: 50μm.

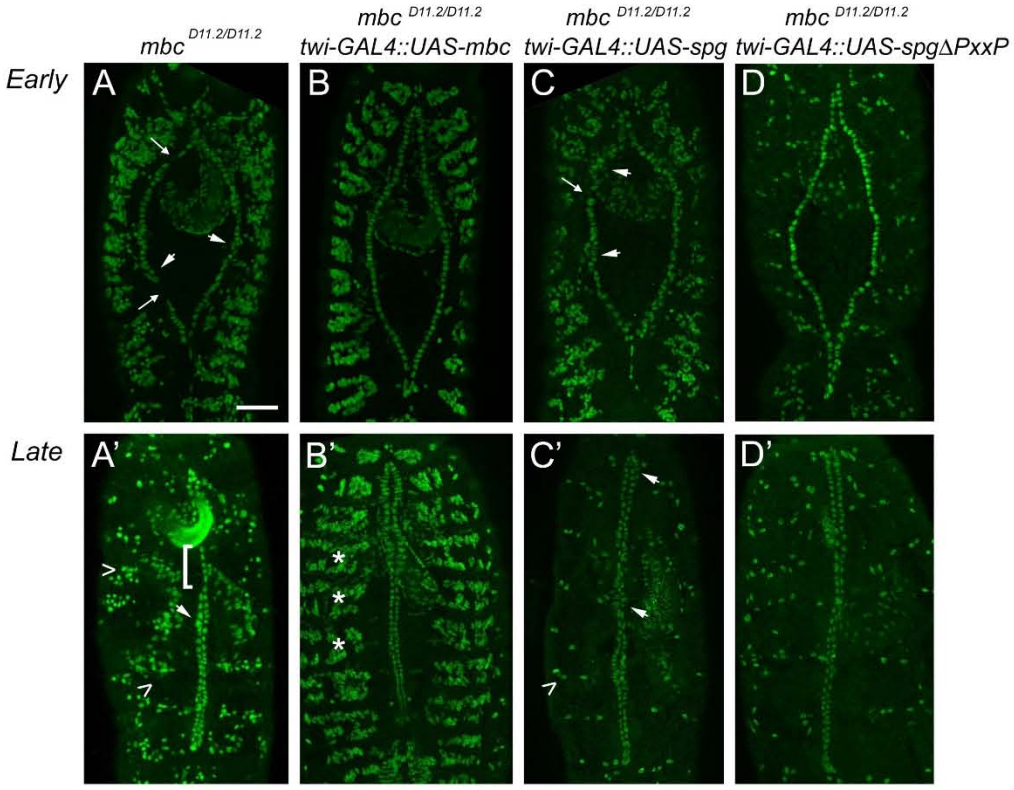

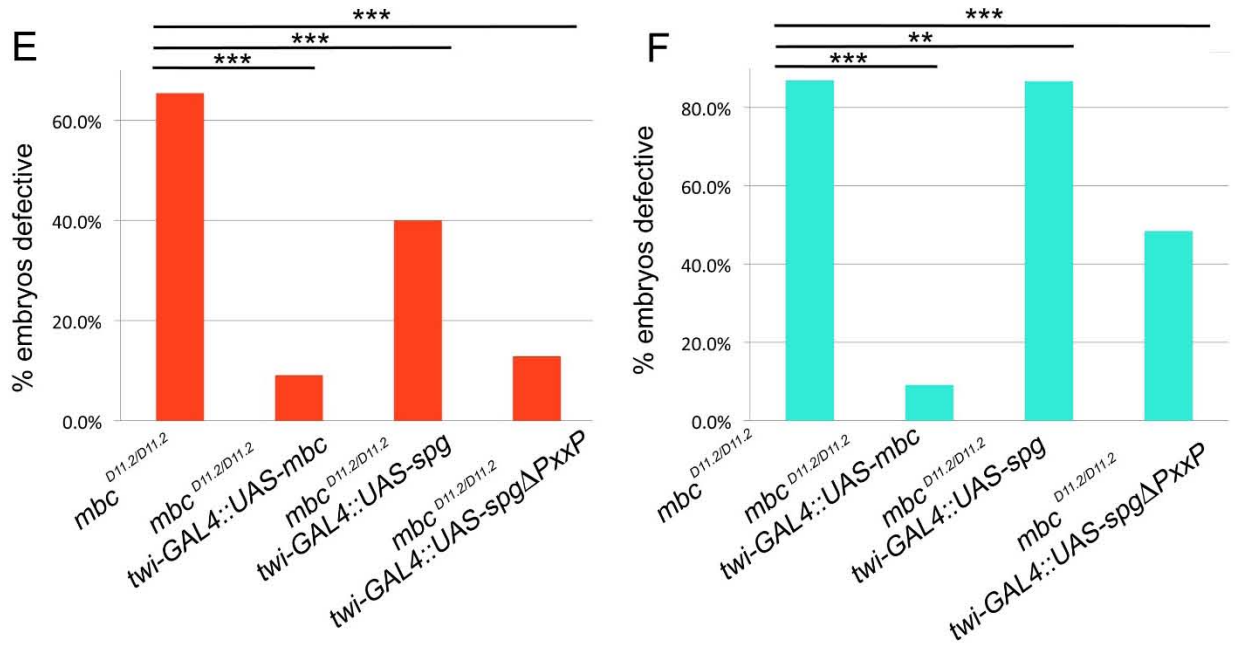

Single rows of cardioblast cells

Clusters of cardioblast cells

*p<0.05
**p<0.01
***p<0.001

Figure 12: *spg* is not capable of rescuing defects resulting from removal of *mbc* in the dorsal vessel (A-C') Early and late stage embryos fluorescently labeled with α-mef2 to visualize muscle nuclei. (A) Removal of *mbc* induces early clustering defects (arrowheads) that often appear next to lateral breaks (arrows). (A') These clustering defects often persist until later in development (arrowheads) where rows of single cells (brackets) are also seen. (B, B') Expression of *UAS-mbc* in an *mbc* mutant background with *twist-GAL4* rescues both early and late defects seen in *mbc* mutants alone. (C, C') No rescue of the *mbc* mutant phenotype is seen upon expression of *UAS-spg.* (D,D') Expression of *UAS-spgΔPxxP,* which removes the C-terminal proline rich region, partially rescues the dv defects in *mbc* mutants, but not the myoblast fusion defects (D', carets). (E,F) Quantitation of the ability of *UAS-spg* to rescue unpaired cardioblasts (E) or cardioblast clusters in st. 17 $mbc^{-/-}$ embryos. Posterior is up for all embryos. Scale bar: 50μm.

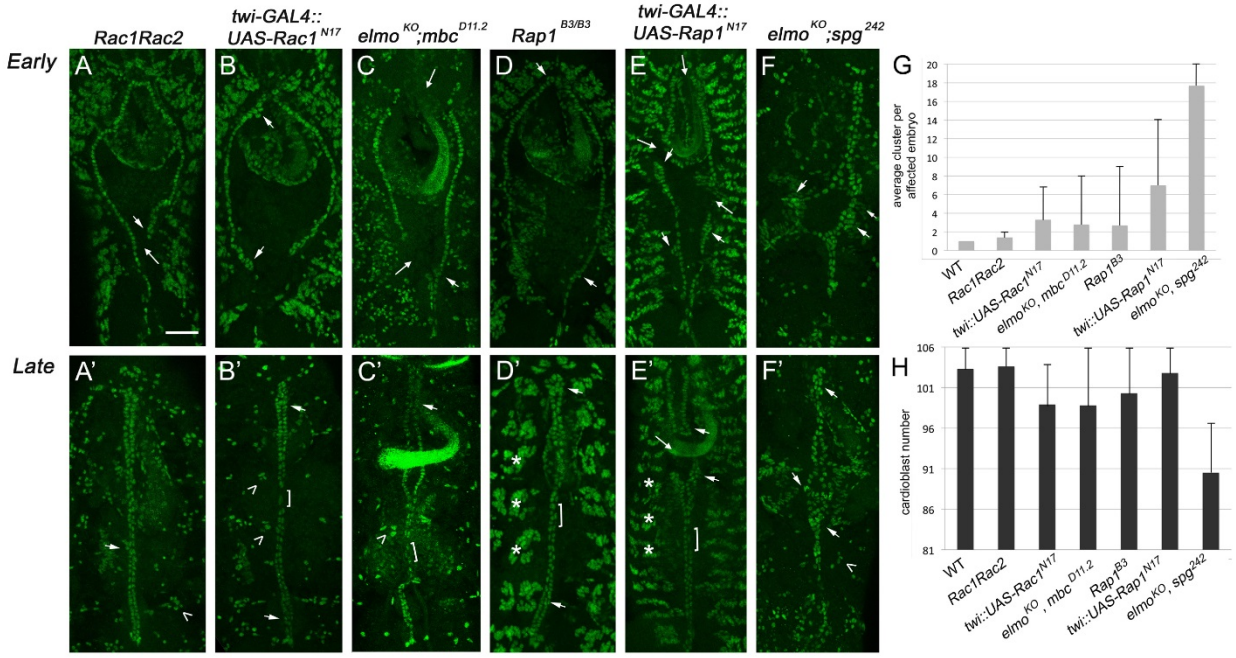

Figure 13: GTPase activation of both Rac and Rap1 is required for correct patterning of the dorsal vessel (A-F') Early and late stage embryos fluorescently labeled with α-mef2 to visualize muscle nuclei. (A-F) Early defects in dv development include lateral gaps (arrows) and clustering (arrowheads). (A'-F') Later in development, these clusters (arrowheads) persist and regions of single cells are present (brackets). (A-C') Inactivation of the Rac GTPase pathway using classical alleles (A, A'), dominant negative overexpression (B, B') or double mutant null alleles of the upstream GEF complex (C, C') results in early lateral breaks, clustering, and regions of single cells in later development indicative of a twist or gap. Note the disorganized muscle nuclei seen in these mutants (carets). (C, C') Removal of the zygotic portion of *Rap* iduces moderate clustering both early and late. (E, E') Overexpression of the constitutively active form of *Rap* causes severe clustering and lateral gaps both early and late. Note the organized muscle nuclei (asterisk). (F, F') Severe clustering is also seen when removing the

zygotic contribution of the *elmo; spg* GEF complex. See Table 2 for quantification. (G,H) Graphs illustrating the average number of clusters per affected embryo (G) or cardioblast number (H) in mutants that alter GTPase activity. Posterior is up for all embryos. Scale bar: 50μm

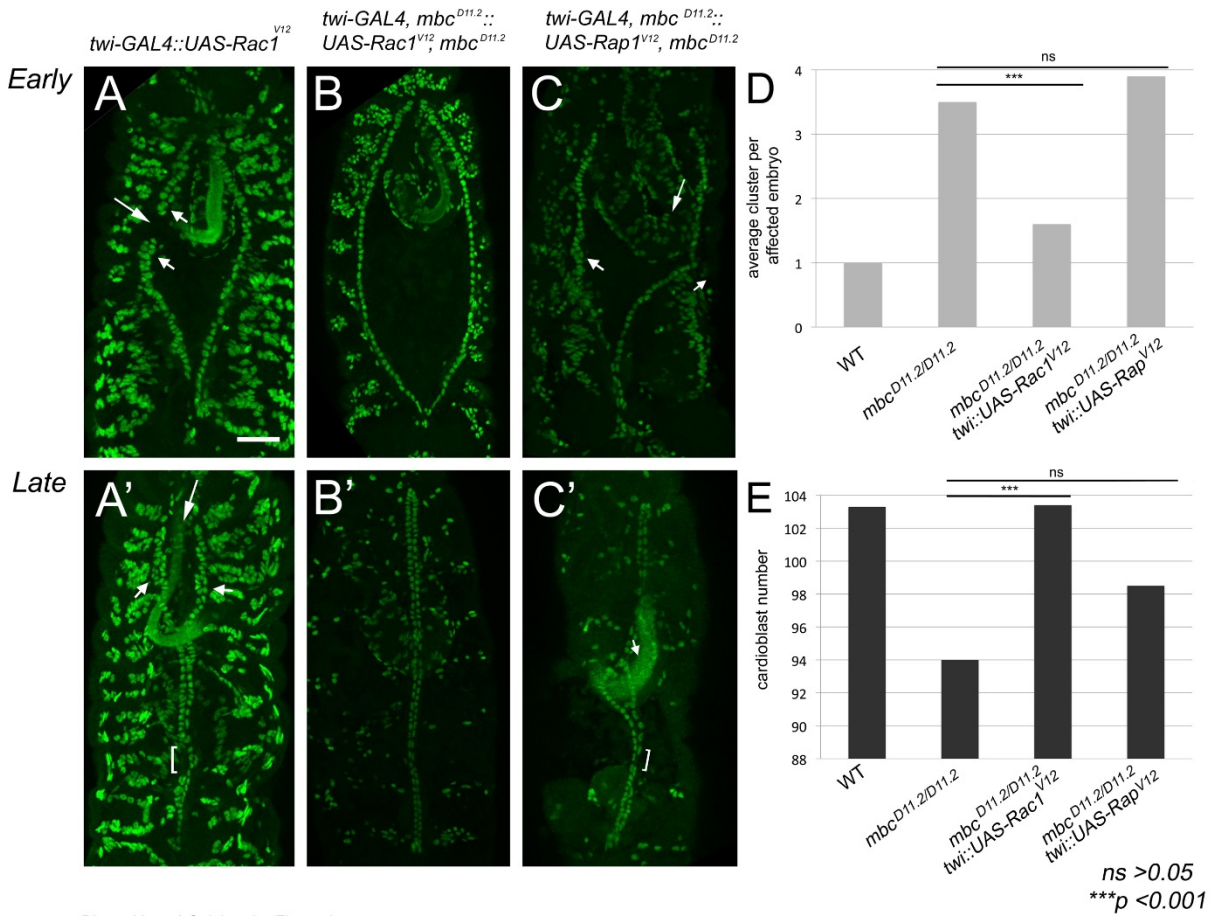

Figure 14: Mbc acts upstream of Rac in the dorsal vessel (A-C') The nuclear marker Mef2 is used to label early and late stage embryos. (A, A') Driving the constitutively active form of *Rac* under control of the *twi* promoter, causes lateral breaks (A, arrows), cardioblast clustering (A, A', arrowheads), posterior openings (A', arrow) and regions of single cells (A', brackets). (C-C') Expression of Rac^{V12} (B,B'), but not $Rap1^{V12}$ (C,C') in an *mbc* mutant background suppresses both early and late clustering defects and eliminates the single cell phenotype (B, B'). (D,E) Comparison of the ability of activated Rac1 or Rap1 to suppress cardioblast clustering (D) or the loss of cardioblast number (E) seen in $mbc^{-/-}$ mutants. Posterior is up for all embryos. Scale bar: 50μm.

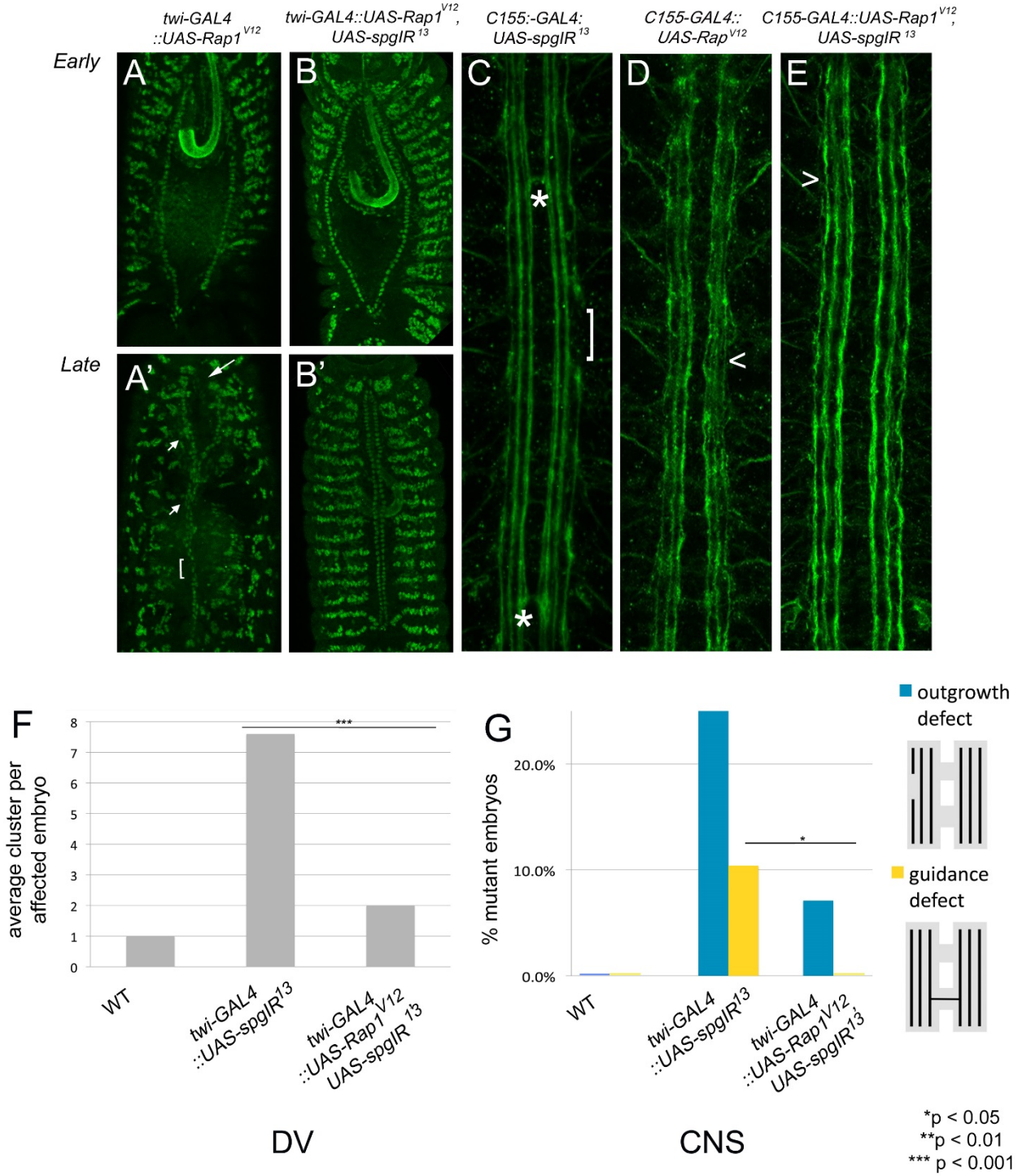

Figure 15: Expression of *Rap*^{V12} can temper *spg*$^{-/-}$ phenotypes (A-E) St. 13 (A,B) or st. 17 (A',B',C-D) C-H) embryos fluorescently-labeled with α-mef2 to visualize muscle nuclei or α-1D4 to label CNS longitudinal axons. (A, A') Embryos solely overexpressing the

constitutively active form of *Rap1* show early and late clustering defects (arrowheads), abnormal posterior openings (arrows), and lateral gaps (brackets). (B,B') All of the dv defects seen when knocking down *spg* levels using an embryonic lethal RNAi line, *spgIR*^{13}, are ameliorated with co-expression of the constitutively active form of *Rap*. (C) RNAi knockdown of *spg* (*UAS-spgIR*^{13}) using the pan neuronal driver, *C155-GAL4*, gives rise to outgrowth defects (brackets) and midline crossovers (asterisks). (D) Overexpression *Rap*^{V12} on its own does not show guidance errors, but instead results in minor unbundling of the longitudinal axons (D, caret). (E) Outgrowth and guidance defects seen when knocking down Spg protein levels by RNAi (C, asterisk and bracket) are rescued when simultaneously expressing *Rap*^{V12}. (F,G) Quantitation of the ability of *UAS-Rap*^{V12} to suppress cardioblast clustering (F) or CNS defects (G) in *spgIR* embryos. Posterior is up for all embryos. Scale bar: 50μm.

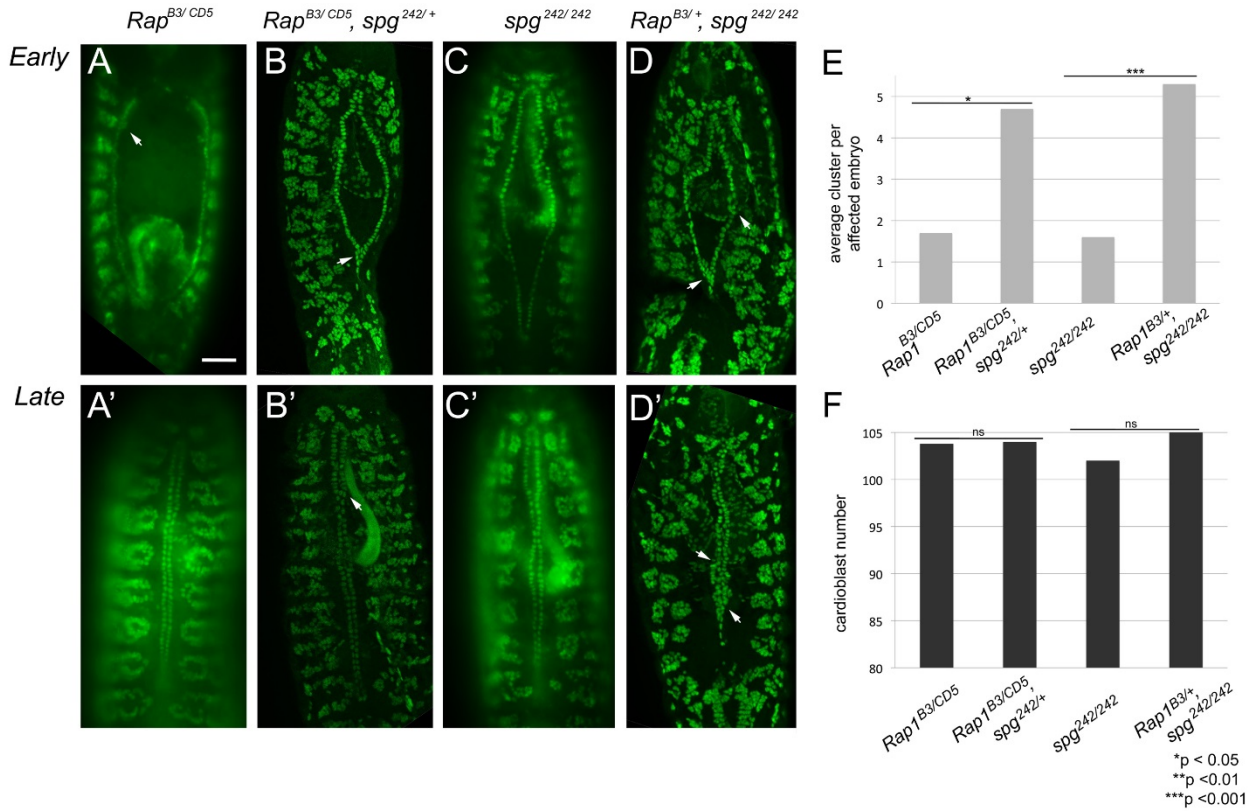

Figure 16: Genetic interactions between *spg* and *Rap1* (A-D') Dorsal views of cardioblast cells stained with Mef2 in early (A-D) and late (A'-D') dv development. The number of cell clusters in *Rap1*$^{-/-}$ (A,A') or *spg*$^{-/-}$ (C,C') mutants is enhanced upon removal of one copy of either of *spg* (C,C') or *Rap1* (D,D'). (E,F) Enhancement of dv clustering phenotypes (E) and a lack of cardioblast numbers (F) in combinations of *spg* and *Rap1* alleles examined at st. 17. Posterior is up for all embryos. Scale bar: 50μm

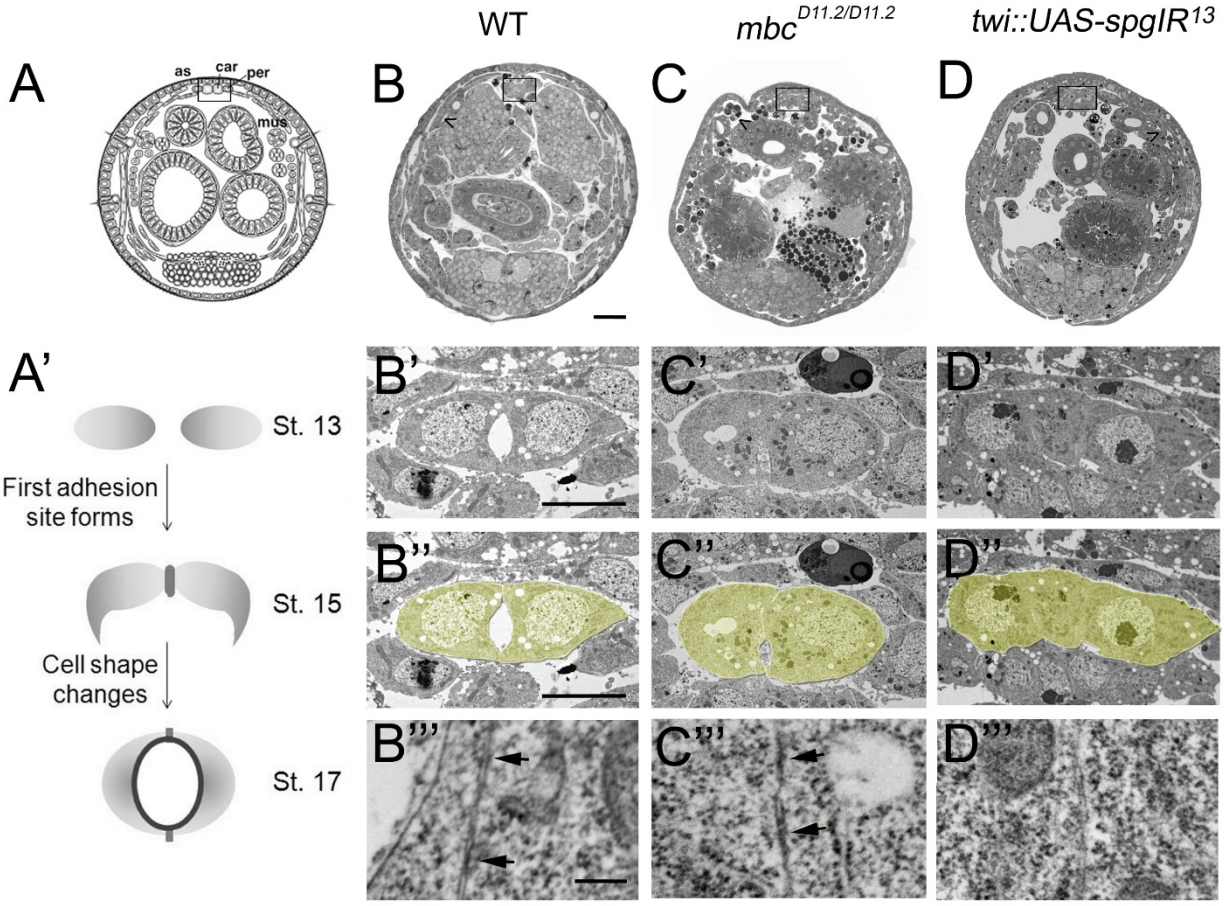

Figure 17: Mbc and Spg are required for proper dv lumen formation (A-D''') Cross sections of the *Drosophila* dv to visualize cardioblast cell shape changes. (A) Schematic representation of a whole mount embryo cross-section. The dv is located on the dorsal side just under the epidermis (box). (A') Schematic representation of dv lumen development from st. 13- st. 17. Two cardioblasts meet at the dorsal midline to create an adhesion site, followed by cell shape changes which allow for the formation of a ventral second adhesion site. This process is coincident with lumen formation, resulting in a linear heart tube through which hemolymph flows. (B-B'') The dv in WT embryos consists of crescent shaped cardioblasts with a large, central lumen. (C-C'') The cardioblasts are rounded and fail to form a lumen in *mbc* mutants. (D-D'') *twi-*

GAL4::UAS-spgIR^{13} embryos also result in lumen formation, although the cardioblasts retain their crescent shape. Note the lack of myoblast fusion seen in *mbc* mutants (C, caret) compared to the fused muscle seen in WT and *spg RNAi* (B, D carets). (B”-D”) High magnification electron micrographs of cardioblast junctions. (B”, C”) Electron dense regions (arrow) indicate the formation of adherens junctions in WT (B’’) and *mbc* mutants (C’’). Electron-dense regions are not observed along the adjacent membranes in *spg IR* embryos (D”). Scale bar: (B-D) 20μm, (B’-D’) 5μm, (B”-D”) 250nm.

Table 2: Phenotypes present in early dorsal vessel development

		Embryos that exhibit clustering (%)	Average clusters/embryo	cardioblast #	(n)
A	*WT*	8.3%	1.0	103.3	48
	24B-Gal4, spg^{242}::UAS-spgRNAi^{353}, spg^{242}	31.0%	2.0	102.7	29
	24B-GAL4::UAS-spgIR^{13}	70.6%	7.1	99.8	34
	twi-GAL4::UAS-spgIR^{13}	78.9%	7.6	99.8	38
B	*$mbc^{D11.2}$*	100.0%	3.5	102.4	17
	twi-GAL4, $mbc^{D11.2}$::UAS-mbc, $mbc^{D11.2}$	43.0%	3.1	103.4	14
	twi-GAL4, $mbc^{D11.2}$::UAS-spg, $mbc^{D11.2}$	88.0%	5.6	104.3	17
	twi-GAL4, $mbc^{D11.2}$::UAS-spgΔPxxP-GFP, $mbc^{D11.2}$	80.0%	2.4	102.8	40
C	*Rac1Rac2*	43.9%	1.4	102.4	21
	twi-GAL4::UAS-Rac1^{N17}	59.3%	3.3	96.7	27
	$elmo^{KO}$; $mbc^{D11.2}$	75.0%	2.8	99.5	13
	Rap1$^{B3/B3}$	62.1%	2.7	101.3	29
	twi-GAL4::UAS-Rap1^{N17}	75.0%	7.0	103.3	32
	$elmo^{KO}$; spg^{242}	91.0%	17.7	98.5	11
D	*twi-GAL4::UAS-Rac1^{V12}*	100.0%	11.5	101.8	13
	twi-GAL4, $mbc^{D11.2}$::UAS-Rac1^{V12}, $mbc^{D11.2}$	53.8%	2.8	102.8	13
	twi-GAL4, $mbc^{D11.2}$::UAS-Rap1^{V12}, $mbc^{D11.2}$	67.9%	3.9	97.9	28
E	*twi-GAL4::UAS-Rap1^{V12}*	40.0%	2.3	101.9	15
	twi-GAL4::UAS-spgIR^{13}, UAS-Rap1^{V12}	34.5%	2.0	103.4	29
F	*$spg^{242/242}$*	41.2%	1.6	104.6	31
	Rap1$^{B3/+}$, $spg^{242/242}$	66.7%	5.3	100.2	18
	Rap1$^{CD5/B3}$	35.3%	1.7	102.8	17
	Rap1$^{CD5/B3}$, $spg^{242/+}$	52.3%	4.7	102.3	29

Table 3: Phenotypes Present in Late Development

		Single cells (%)	Embryos that exhibit clustering (%)	Average clusters/ embryo	cardioblast #	(n)
A	*WT*	11.1%	14.8%	1.3	103.3	54
	24B-GAL4, spg^{242}::UAS-spgRNAi^{353}, spg^{242}	9.7%	12.9%	1.0	102.9	31
	24B-GAL4::UAS-spgIR^{13}	29.4%	35.0%	5.5	101.4	17
	twi-GAL4::UAS-spgIR^{13}	21.4%	53.6%	5.5	99.6	28
B	*mbc$^{D11.2}$*	65.4%	86.9%	3.3	94.0	42
	twi-GAL4, mbc$^{D11.2}$::UAS-mbc, mbc$^{D11.2}$	9.1%	9.1%	2.5	101.0	22
	twi-GAL4, mbc$^{D11.2}$::UAS-spg, mbc$^{D11.2}$	40.0%	86.7%	4.0	96.2	15
	twi-GAL4, mbc$^{D11.2}$::UAS-spgΔPxxP-GFP, mbc$^{D11.2}$	12.9%	48.4%	2.3	100.4	34
C	*Rac1Rac2*	0.0%	5.3%	3.0	103.6	19
	twi-GAL4::UAS-Rac1^{N17}	26.5%	41.2%	2.6	98.9	34
	elmo^{KO}; mbc$^{D11.2}$	50.0%	75.0%	2.3	98.8	17
	Rap1$^{B3/B3}$	10.7%	17.4%	2.9	100.3	28
	twi-GAL4::UAS-Rap1^{N17}	54.5%	30.3%	7.6	102.8	33
	elmo^{KO}; spg^{242}	60.0%	100.0%	3.8	90.50	4[a]
D	*twi-GAL4::UAS-Rac1^{V12}*	100.0%	100.0%	7.5	105.5	2[a]
	twi-GAL4, mbc$^{D11.2}$::UAS-Rac1^{V12}, mbc$^{D11.2}$	0.0%	62.5%	3.2	103.0	16
	twi-GAL4, mbc$^{D11.2}$::UAS-Rap1^{V12}, mbc$^{D11.2}$	25.0%	25.0%	2.0	98.5	4[a]
E	*twi-GAL4::UAS-Rap1^{V12}*	46.2%	100.0%	10.2	106.5	16
	twi-GAL4::UAS-spgIR^{13}, UAS-Rap1^{V12}	3.2%	25.8%	2.5	102.1	31
F	*spg$^{242/242}$*	5.0%	20.0%	1.5	103.8	20
	Rap1$^{B3/+}$, spg$^{242/242}$	1.1%	44.4%	5.6	105.1	9
	Rap1$^{CD5/B3}$	0.0%	14.3%	1.0	104.0	7
	Rap1$^{CD5/B3}$, spg$^{242/+}$	8.9%	30.0%	6.0	102.0	16

[a] These genotypes resulted in low numbers of surviving progeny after st. 13.

CHAPTER 4

MATERIALS AND METHODS

Genetics

Fly stocks were raised on standard cornmeal medium at 25ºC unless otherwise indicated. Oregon R was used as the wild-type strain. The following alleles/fly stocks were used: *elmo*^{19F3}, *P{ry[+7.2]=neoFRT}40A* (Geisbrecht, et al, 2008); *elmo*^{PB}, *P{ry[+7.2]=neoFRT}40A* (Geisbrecht, et al, 2008); *elmo*^{KO} (Bianco, et al, 2007); *spg*^{242} (kindly provided by Eyal Schejter); *mbc*$^{D11.2}$ (Erickson, et al, 1997); *Ncad1*^{omb405} (Yonekura, et al, 2007); *Ncad*$^{\Delta 14}$ (Prakash, et al., 2005); *UAS-mbc* (Balagopalan et al., 2006), *UAS-elmo* (Geisbrecht et al., 2008); *UAS-spg* (Biersmith et al., 2011); *UAS-spgIR*^{13} (Eguchi et al., 2013); *UAS-spgRNAi*^{353} (Harvard TRiP Project, BL35396); *spg*^{242} (Biersmith et al., 2011); *Rap1*^{B3} (Biettner et al., 2003); *UAS-Rap1*^{N17} (Boettner et al., 2003); *UAS-Rap1*^{V12} (Hariharan et al., 1991); *elmo*^{KO} (Blanco et al., 2007); *Rap1*^{CD5} (Boettner et al., 2003). *elmo*$^{PB.mat}$ mutants were created as previously described (Geisbrecht, et al, 2008). The following stocks were generated by standard meiotic recombination and isolated on the basis of their failure to complement other alleles, PCR, and/or sequencing to verify the molecular lesion: *spg*^{242}, *mbc*$^{D11.2}$; *elmo*^{19F3}, *Ncad*$^{\Delta 14}$, *elmo*^{KO}; *spg*^{242} and *Ncad*$^{\Delta 14}$; *mbc*$^{D11.2}$, *UAS-spg. mbc*$^{D11.2}$ (for rescue), *UAS-Rap1*^{V12}, *UAS-spgIR*^{13} (for rescue), *24B-GAL4, spg*^{242}, *spgRNAi*^{353}, *spg*^{242}, and *UAS-Rap1*^{V12}, *mbc*$^{D11.2}$ (for rescue). All rescue experiments were performed at 29°C or 30ºC with the exception of *twi-GAL4, UAS-mbc*$^{D11.2}$*::UAS-mbc, mbc*$^{D11.2}$, which was performed at 18ºC. Additional stocks were generated by standard fly crosses.

In situ hybridization and Immunostaining

Embryos were collected on agar-apple juice plates and aged at 25°C. For *in situ* analysis, multiple internal sequences encoding *spg* were transcribed with Sp6 using the DIG mRNA labeling kit (Roche) and hybridized as described [27]. The C-terminal 534AA of Spg were cloned into the pT7HMT expression vector and soluble protein was purified as described [67]. The resulting protein was injected into guinea pigs and antisera was used at 1:500. For immunohistochemistry, embryos were fixed and stained as described [27]. The musculature was visualized using anti-MHC (1:500). The CNS was labeled using mAb 1D4 (1:100, Developmental Studies Hybridoma Bank, University of Iowa) and mAb BP102 (1:20, Developmental Studies Hybridoma Bank, University of Iowa). Secondary antibody was goat anti-mouse-HRP (1:200, Jackson). Fluorescent immunostaining was performed as previously described in Geisbrecht, et al. Primary antibodies used were anti-Repo (1:50, Developmental Studies Hybridoma Bank, University of Iowa) and anti-Slit (1:50, Developmental Studies Hybridoma Bank, University of Iowa) and detected fluorescently using Alexa Fluor 488 goat anti-mouse IgG at 1:400 (Molecular Probes, Carlsbad, CA). Tyramide staining was used to enhance Spg signal for immunofluorescent stainings (Vector Labs, Burlingame, CA). Fluorescent images were collected on Olympus Fluoview 300, Zeiss LSM 710, or Nikon Eclipse 90i and figures were assembled using Photoshop. All statistics were performed using the student t-test. P-values are indicated in each figure.

Mass spectrometry identification and immunoprecipiations

Mass spectrometry experiments were described previously [27]. For immunoprecipitations, ELMO-HA-tagged and untagged transgenic flies were crossed to *mef2-GAL4* females and 6-18h embryos were collected on agar-apple juice plates at 25°C. Embryos were dechorionated and homogenized in lysis buffer [60mM Tris (pH 7.5), 80mM NaCl, 6mM EDTA (pH 8.0), 2% Triton X-100, 1mM Na_3VO_4, 5mM 1-Naphthyl phosphate potassium salt, 2mM PMSF, 2 ug/ml Leupeptin, 2 ug/ml Pepstatin]. The NaCl concentration was increased to 300mM and resulting lysate mixed with anti-HA resin overnight at 4°C. The resin was washed 3 times with wash buffer plus protease inhibitors, boiled in 6x sample buffer and submitted to SDS-PAGE and subsequent Western blotting. The following primary antibodies were used for immunoblotting: anti-Spg (1:1000, this paper), anti-ELMO (1:1000) and anti-HA-HRP (1:2000, Roche). After incubation with goat anti-guinea pig-HRP (Jackson), proteins were visualized with ECL Plus (Amersham).

Molecular Biology

The PxxP region of Spg was determined by primary sequence alignment with Mbc, Dock 180, Dock3 and Dock4 using Multalign. The following primers were designed after secondary structure prediction analysis to reduce the possibility of interfering with protein structure: *forward:* 5'-GCCATTCCCCGGGGAGCTCCCATTC-3' *reverse:* 5'-ATAGTTTAGCGGCCGCTCAGGTA-3'. The *spgΔPxxP* cDNA sequence was generated by amplifying the correct portion of the *spg* cDNA from the full-

length clone (BIERSMITH *et al.* 2011) and out into the pUAST vector. Transgenic flies were produced by Genetic Services, Inc. using standard techniques

Electron Microscopy and Live Imaging

Embryos were prepared for electron microscopy as described (Soplop et al., 2009) and sent to the Saint Louis University Microscopy Core for sectioning, low magnification light micrographs and high magnification electron micrographs.

Constructs

A full length *spg* cDNA sequence was generated by analyzing multiple, overlapping fragments generated by RT-PCR using S2 cells and 0-6 h embryos as a reference source. A full length cDNA was generated by Epoch Biolabs and cloned into pUAST. Transgenic flies were produced by Genetic Services, Inc. using standard techniques.

S2 Cell Transfections

Transient calcium phosphate transfections of pRmHA3-Ncadherin (from) were carried out with $1.2x10^6$ cells/ml and 7-15 ug DNA as needed. Cells were induced 24 hours after transfection with 0.7 μM $CuSO_4$. After 48 hrs, cells were resuspended at a concentration of $1.2x10^6$ cells/ml in 2 mls of BBS buffer (10mM HEPES, 55 mM NaCl, 40mM KCl, 15 mM $MgSO_4$, 20 mM glucose, 50 mM sucrose, and 10 mM $CaCl_2$). The cells were agitated in a 35 mm dish at 100 rpm for 1 hr. The cells were plated on poly-L-lysine coated coverslips and fixed for 10 minutes in 4% PFA in Ca^{2+} and Mg^{2+}-free

(CMF) C& GBS (55 mM NaCl, 40 mM KCl, 10 mM Tricine (pH=6.9), 20 mM glucose, 50 mM sucrose) + 1 mM $CaCl_2$. Standard immunofluorescent protocols were followed using rat anti-Ncad (1:20, Developmental Studies Hybridoma Bank, University of Iowa) and gp anti-Spg (1:500). Secondary antibodies used were Fluor 488 goat anti-rat IgG and Fluor 546 goat anti-guinea pig at 1:400 (Molecular Probes, Carlsbad, CA).

CHAPTER 5

CONCLUSION

Identification and characterization of Spg, a Dock family member

We identified peptides corresponding to the uncharacterized protein CG31048 in an *in vivo* mass spectrometry approach to identify Elmo-binding partners. The *CG31048* locus, which encodes for Sponge, is a member of the growing family of *Drosophila* Dock family proteins. This report is the second identification of a Dock family member in flies since the role of Mbc was uncovered in 1997 [20]. The 11 vertebrate Dock proteins identified thus far can be divided into subgroups based upon primary sequence analysis and GTPase target specificity for either Rac or Cdc42 [5, 6, 38]. In the first group, the Dock-A family consists of Dock180, Dock2, and Dock 5, while the Dock-B subfamily is comprised of Dock3 and Dock4. In flies, this redundancy is simplified with the 2 Dock family members, Mbc and Spg, whom are members of the Dock-A and Dock-B groups, respectively. All of the above family members contain an N-terminal SH3 domain, 2 internal DHR (CZH) domains and a variable C-terminal proline-rich region. Furthermore, they function as unconventional guanine nucleotide exchange factors (GEFs) for the GTPase Rac. Members of the Dock-C (Dock 6, Dock7, Dock8) subfamily and Dock-D (Dock9, Dock10, Dock11) subfamily bind to the GTPase Cdc42. The 2 orthologous Drosophila proteins, CG42533/Dm ziz (Dock-C) and CG11376/Dm zir (Dock-D) have not yet been characterized in flies.

Alleles of *spg* were originally identified in a maternal effect screen and later characterized for their role in actin-dependent events in early *Drosophila* embryogenesis

[35, 36]. Our mRNA and protein expression analysis suggested Spg may be required after cellularization due to strong expression in the visceral mesoderm, dorsal vessel, and developing ventral nerve cord. As removal of the maternal contribution of *spg* null alleles results in lethality, the role for *spg* in later developmental processes had not been examined. However, the identification of Spg as an Elmo-interacting protein gave us insight into how to examine the role of Spg in late embryogenesis using double mutant analysis. While zygotic single mutants of *spg* and *elmo* appeared essentially wild-type, removal of both the zygotic contribution of both *spg* and *elmo* resulted in axonal patterning defects. Obtaining a phenotype in these double mutants was especially convincing as both *elmo* and *spg* are maternally-loaded components. As mentioned above, removal of either *spg* or *elmo* maternal contribution results in early embryonic lethality [21]. As *spg* has shown to be required for early actin cap and metaphase furrow formation, it is fair to hypothesize that that these two genes may function in concert in early embryo development, where Mbc is not required.

Downstream GTPase of the Dock-Elmo complexes

Vertebrate Dock 4 was originally identified as a CDM family member capable of activating the small GTPase Rap1 in GTPase pull-down assays [66]. Functionally, a deletion of endogenous Dock4 in osteosarcoma cells was shown to rescue the formation of adherens junctions and could be suppressed by co-expression of dominant-negative Rap1 [66]. Recent studies have demonstrated that Dock 4 is also capable of activating the GTPase Rac1 [39, 67, 68]. This data suggests that GTPase activation of either Rac and/or Rap1 by the Spg-Elmo complex is context and/or tissue-dependent. Our model for Dock-

Elmo function in embryogenesis is shown in Figure 8. Only the Mbc-Elmo complex functions in the developing musculature to activate the GTPase Rac. While it is clear that regulation of the actin cytoskeleton is downstream of the Mbc-Elmo→Rac signaling pathway, the upstream receptors that mediate this signaling are unknown. Our data suggests that both Mbc and Spg function in the *Drosophila* developing nervous system. All literature thus far supports a model whereby the Mbc-Elmo complex activates Rac. Alternatively, the Spg-Elmo complex may regulate Rac and/or Rap1 activity. If both the Mbc-Elmo and Spg-Elmo protein complexes function upstream of Rac, they may be acting redundantly to regulate Rac-dependent actin cytoskeletal changes. Alternatively, the downstream effector functions of Rac activity may lead to changes in cell-cell adhesion or may be mediated through the GTPase Rap1. We hypothesize that differences in the C-terminal proline-rich regions of Mbc and Spg may be responsible for their differential activities. In myoblast fusion, the proline-rich region of Mbc is not required [8]. However, Spg and vertebrate Dock3/4 contain additional proline-rich sites not present in Mbc/Dock180. Further experiments will be necessary to define the cellular and molecular mechanisms necessary to carry out Dock-Elmo functions in the developing CNS.

Regulation of GEF activity

Elmo expression is ubiquitous throughout fly development, while Mbc and Spg expression is predominate in the muscle and nervous system, respectively. Based upon the tissue-specific expression patterns of Mbc and Spg, we originally hypothesized that complementary expression patterns may be one mechanism for the tissue-specific

regulation of Rac activation through the Dock-Elmo complexes. However, our results indicate that the role of Mbc-Elmo and Spg-Elmo is more complicated. While the Mbc-Elmo complex seems to be the primary GEF complex for Rac activation in the musculature, both the Mbc-Elmo and Spg-Elmo complexes may both be necessary to correctly pattern axons in the developing central nervous system. In support of the idea that both complexes are required in certain developmental situations, the Rorth lab found that both Spg and Mbc are required in border cell migration [37]. Removal of both Spg and Mbc function in the border cells phenocopies loss of Elmo, suggesting that these 2 genes function in concert with Elmo to guide migration. Further experiments are required to determine if the observed CNS defects in *spg* and *mbc* mutants are autonomous in the nervous system. Alternatively, axonal patterning defects observed in *mbc* mutants may be a secondary consequence due to a requirement for Mbc in the musculature.

In the musculature, the only known GEF shown to be required for Rac activation is the Mbc-Elmo complex. However, in the developing nervous system, in addition to the unconventional Dock-Elmo complexes, the conventional GEFs Trio and Sos are required [69-71]. It is not clear how these multiple GEFs are regulated throughout CNS development. Possible mechanisms include the: (1) regulation of GEF expression either in subsets of specific neurons or precise subcellular localization within the same neuron; (2) unique physical associations between GEFs and receptors specific for distinct steps in axonal patterning; and (3) regulation of GEF activity via post-translational modifications including phosphorylation or ubiquitination. While these ideas have not been examined in detail for all known GEFs, what is known is discussed below.

First, it is possible mechanisms exist within the cell or tissue to compartmentalize GEF function as the spatial expression patterns of all GEFs in the developing ventral nerve cord seems to be fairly broad. Mbc is expressed at low or undetectable levels with reagents currently available, while Spg is expressed in all commissural and longitudinal axons, but not glial cells. Likewise, Sos protein is broadly expressed in many cell types around stage 12 and becomes enriched in CNS axons [71]. While Trio is expressed in axons that run on longitudinal tracts and those that cross the midline, enrichment of this protein is evident in the longitudinal fascicles [69]. Trio is largely localized near the membrane [72], while cytoplasmic Spg and Sos can be recruited to the membrane by their association with N-cadherin and Robo, respectively [71]. It is not yet clear if membrane recruitment is sufficient to promote Rac activation, or if conserved mechanisms exist to activate GEFs where their activity may be needed. For example, by binding to RhoG, Elmo can target Dock180 to the membrane [13]. In addition, Elmo binding to Dock180 relieves a steric inhibition by exposing the DHR-2 domain of Dock180 that binds Rac [12]. This remains to be shown for other Dock family members.

Next, it is possible that each distinct step of neuronal pathfinding requires a unique set of proteins that allow upstream receptors to signal to downstream proteins for a specific biological output. For example, Trio cooperates with the Abelson tyrosine kinase (Abl) to promote Rac-dependent actin cytoskeletal dynamics in Frazzled-mediated commissure formation [73]. In the separate process of longitudinal fascicle formation, a trimeric complex of Robo-Dock-Sos activates Rac to promote axon repulsion [71]. Separately, N-cadherin is suggested to be required for fasciculation and directional growth cone migration [43]. Thus, the Ncad-Dock-Elmo complex may be responsible for

this latter aspect of axonal pathfinding, while other steps may be mediated by individual receptor-GEF complexes. However, additional evidence suggests this regulation may be more complex. Preliminary data from our laboratory demonstrates that Ncad may genetically interact with other Rac GEFs to affect earlier CNS development and later axon pathfinding results (Biersmith, B. and Geisbrecht, E.; unpublished data). Dock180 binds the vertebrate receptor Deleted in Colorectal Cancer (DCC) (similar to the Netrin receptor Fra in flies) [74]. In addition, inhibition of Dock180 activity decreased the activation of Rac1 by Netrin [50]. Another study suggests that Robo is required for multiple, parallel pathways in axon guidance and activated Robo function inactivates N-Cadherin-mediated adhesion [66]. Current models suggest activated Robo binds to Abl and N-cadherin, thus providing a mechanism to weaken adhesive interactions during fasciculation to allow for mediolateral positioning of axons along the ventral nerve cord. The association of either Mbc or Spg proteins in the Netrin signaling pathway has not been examined. So far, we have not observed significant differences in genetic combinations that remove *elmo* with either *robo* or *slit* function in midline crossing (Lui, Z. and Geisbrecht, E.; unpublished data). Furthermore, no significant increases in midline guidance errors were observed in $Ncad^{\Delta 14}$*; elmo* mutants, suggesting that Ncad and Spg may function in this process independent of Elmo function. It is clear that additional analysis of Robo and N-Cadherin dynamics are needed in the well-established CNS fly model to determine their *in vivo* relevance.

Finally, the physical interactions of GEF proteins with specific membrane receptors may allow the GEFs to be in a unique subcellular localization for post-translational modifications that regulate activity. As mentioned above, Dock180 is

capable of binding and activating Rac when sterically relieved upon Elmo binding [12]. In addition, the presence of Elmo1 inhibits the ubiquitination of Dock180, thus stabilizing the amount of GEF available to activate Rac [75]. Finally, although the significance is unclear, Dock180 is phosphorylated upon Integrin binding to the extracellular matrix [76]. Trio has also been shown to be tyrosine phosphorylated upon co-expression with Abl [73], suggesting this may be a common mechanism for GEF regulation. Elmo is also phosphorylated on tyrosine residues [77], providing another level of GEF regulation. Further experimentation must be done to determine whether these modifications of GEFs also lead to regulation of Rac activity.

We have used various tissues that form in *Drosophila* embryonic development, including the somatic muscle, CNS, and heart tube, to discern underlying differences of GEF family member function in cell morphogenic events. In the present study, we demonstrate that Mbc and Spg appear to have independent roles in most tissues examined. First, expression of Spg in the somatic muscle cannot compensate for loss of Mbc during myoblast fusion. Second, while both Mbc and Spg are required for dv development, they affect different aspects of morphogenesis. Loss of *mbc* results in small clusters of cardioblast cells (3.3-3.5 cells/cluster) breaks in the contralateral rows of adjacent cells, and a total loss of about 10 cardioblast cells per embryo. These phenotypes are distinct from knockdown of *spg* using RNAi, where the primary defect is larger clusters of multilayered cardioblast cells (5.5-7.6). As a better readout of cell morphogenic events, ultrastructure analysis of opposing cardioblast cells reveal that cell shape changes do not occur in $mbc^{-/-}$ mutants, while a decrease in *spg* allows the cells to maintain an elongated shape. Loss of both Mbc and Spg affect lumen formation, but differentially affect the

ability of putative adhesion sites to form. Taken together, this data provides strong evidence for differential roles of Mbc and Spg *in vivo.*

Dock protein specificity

Discrepancies concerning the downstream GTPase target(s) of the Dock family of GEFs have existed for about ten years[1, 2]**.** Numerous 19 reports demonstrate that both proteins of the Dock-A & B family, specifically Dock180/Mbc and Dock3 and 4/Spg, can activate Rac1 in *in vitro* GTPase activation assays[39, 66, 68]. *In vivo*, it is well-established that Dock180/Mbc activates Rac in all contexts examined[20, 21, 49, 78], while the data for Dock4/Spg are less clear. A substantial body of evidence links Dock3 and Dock4 to the activation of Rac in both neuronal tissues and cancer cells[39, 79 30], primarily through Rac-dependent actin rearrangement in axon outgrowth or cellular metastasis. Consistent with Rac being the primary downstream target of Dock proteins, Mbc and Spg are thought to function redundantly upstream of Rac1 in *Drosophila* border cell migration[33].

Two reports suggest an alternative or additional role for Dock-B family members in the activation of Rap1. The first evidence emerged about ten years ago when Yajnik and colleagues showed that Dock4 is capable of activating Rap1 in GTPase activation assays[66]. Recent studies also provide supportive evidence for Rap1 activation via Spg in the differentiation of R7 photoreceptor cells in the *Drosophila* eye[28]. Duolink *in situ* PLA experiments suggest a physical interaction between Spg and Rap1 at the plasma membrane in photoreceptor cells. The authors also rule out Rac as an effector of Spg in R7 photoreceptor differentiation. A reasonable explanation for these apparently conflicting results is that Dock-B proteins may exhibit dual roles in the activation of both Rac and Rap1, dependent on cellular context.

Nucleotide exchange of GDP for GTP is catalyzed by the DHR2 domain in unconventional Dock family members. A conserved valine residue within the α10 helix of DHR2 acts as a nucleotide sensor that senses and destabilizes bound GDP. Subsequent binding of GTP results in 20 a conformational change and release of the activated GEF[80]. However, the mechanisms that mediate GTPase specificity within each DHR2 domain is not known. So what is the importance of the C-terminal proline-rich region and why does it possess the most divergent sequence conservation between Dock-A and Dock-B family members?

There is some evidence to suggest that the C-terminal part of Dock4 may be required for GTPase specificity. An identical point mutation (Pro1718Leu) in *Dock4* was identified in two independent cell lines, one derived from prostate cancer and the other from ovarian cancer. While in these experiments Dock4-WT preferentially activates Rap1 in *in vitro* activation assays, the presence of the Dock4-Pro1718Leu mutation altered the GTPase specificity for Rac and Cdc42. Expression of this mutated version in mouse 3081 osteosarcoma cells showed a decrease in actin stress fibers and the presence of filopodia, an observation consistent with altered GTPase activation. Contact inhibition is not a normal feature of this osteosarcoma cell line and staining of these cells with β-catenin do not show the presence of adherens junctions. Transfection with Dock4-WT results in the appearance of intercellular adherens junctions. No such effect is observed upon co-expression of Rap1N17 in this Dock4-WT background or independent expression of Dock4-Pro1718Leu[66].

Our observations are consistent with this putative role for the C-terminal proline-rich region of Spg in dv morphogenesis. Expression of Spg deleted for the entire PxxP

region (*UAS- spgΔPxxP*) is able to suppress *mbc*-mediated single cell stretching and cardioblast clustering defects, while overexpression of full-length Spg does not. Interestingly, neither version of Spg can rescue myoblast fusion defects due to loss of *mbc,* suggesting that Spg exerts it effects only in tissues where both proteins are known to function. While we do not yet understand the role of the PxxP region, whether in GTPase specificity and/or binding to other SH3 domain-containing 21 proteins, it is worth noting that Spg contains four additional putative PxxP-binding sites not present in Mbc[29].

Cardioblast cell shape changes in lumen formation

We chose the dv as a two-cell system to better understand whether Mbc and Spg influence the same or independent cell morphogenic effects. Examination of dv development in whole mount embryos allows us to determine whether Dock proteins are required for cardioblast number and to note the patterning of cardioblast cells along the anterior-posterior axis. In contrast, analysis of TEM cross-sections through the dv highlight actin-mediated cell shape changes and the presence of putative adherens junctions. As shown in Fig. 9A, the prevailing model for cardiac lumen formation involves the coordination of both cell shape changes and lumen formation (SANTIAGO-MARTÍNEZ *et al.* 2006; MEDIONI *et al.* 2008; ALBRECHT *et al.* 2011). These events occur after formation of the first junctional domain at the future dorsal positon of the dv. Our current data is consistent with the canonical role of Mbc in actin cytoskeletal rearrangement through the Rac GTPase. Expression of constitutively-active Rac suppressed dv patterning defects present upon loss of Mbc. Furthermore, the cardioblast cells in $mbc^{-/-}$ mutants properly migrate to the dorsal midline and are able to form

adhesion sites, as indicated by the presence of electron-dense plaques between the cardioblast membranes. However, the cardioblast cells remain rounded, likely due to the inability of actin-mediated cytoskeletal events. Perhaps *mbc* mutants lack the ability to make these shape changes, thus resulting in an extended junctional domain. We postulate that Spg is required for Rap1 activation to regulate adherens junctions formation. A genetic interaction between *spg* and *Rap1* regulates apsects of cardioblast patterning, 22 namely the multilayering of heart cells within a contralateral row. TEM analysis shows that *spg RNAi* mutants lack electron-dense accumulations along adjacent cardioblast membranes, suggesting defects in the ability to form the first junctional domain. However, the cardioblasts are not rounded as in *mbc* mutants, but appear elongated, suggesting that actin-mediated cell shape changes are not affected. We cannot rule out the possibility that Spg could be affecting Slit/Robo signaling at the luminal membrane, thus resulting in an inhibition of Armadillo/DE-Cadherin accumulation at adherens junctions and an increase in the regulation of actin-mediated cytoskeletal events[64].

Here, we have shown that the genetically tractable model organism *Drosophila melanogaster* can provide an excellent *in vivo* system to study the cellular behavior of Dock proteins, which have already been implicated in a vast array of diseases in mammals, including developmental limb disease, congenital cognitive disorders, progressive cancers, and neurodegenerative diseases. Understanding the function of these proteins at the cellular level during development will likely aid in the understanding of their roles in this spectrum of biological processes.

In conclusion, our analysis of *Drosophila* dv morphogenesis provides evidence for differential roles of the Dock family members Mbc and Spg in regulating either cell

shape changes or adhesion dynamics during lumen formation. Future experiments will be directed at identifying other proteins that regulate GEF function in tissues where both Mbc and Spg are required for cellular processes.

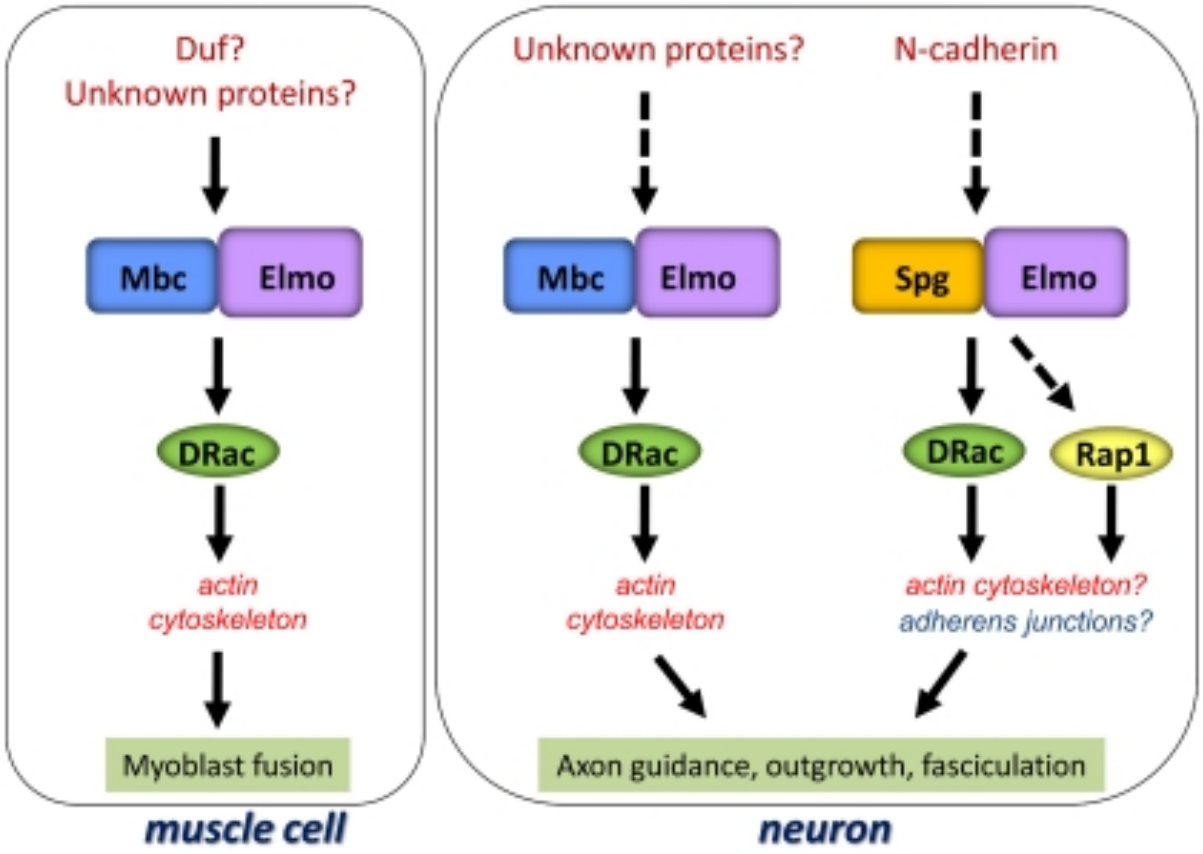

Figure 18: Model of CDM-ELMO Pathway In the muscle, Mbc is the sole CDM family member that functions with Elmo to mediate cytoskeletal modifications through the GTPase Rac (left panel). In a neuronal cell (right panel), both Mbc and Spg contribute to nervous system formation. In this model, the Mbc-Elmo complex is downstream of yet unidentified proteins and presumably signals through Rac. In contrast, our data suggests Spg-Elmo may function downstream of Ncad. The target of the Spg-Elmo complex, is unclear.

REFERENCE LIST

Works Cited

1. Laurin, M.; Côté, J. F., Insights into the biological functions of Dock family guanine nucleotide exchange factors. *Genes Dev* **2014,** *28* (6), 533-47.
2. Gadea, G.; Blangy, A., Dock-family exchange factors in cell migration and disease. *Eur J Cell Biol* **2014**, *93* (10-12), 466-477.
3. Cherfils, J.; Zeghouf, M., Regulation of small GTPases by GEFs, GAPs, and GDIs. *Physiol Rev* **2013,** *93* (1), 269-309.
4. Friedl, P.; Gilmour, D., Collective cell migration in morphogenesis, regeneration and cancer. *Nat Rev Mol Cell Biol* **2009,** *10* (7), 445-57; Steeg, P. S., Tumor metastasis: mechanistic insights and clinical challenges. *Nat Med* **2006,** *12* (8), 895-904.
5. Cote, J. F.; Vuori, K., GEF what? Dock180 and related proteins help Rac to polarize cells in new ways. *Trends Cell Biol* **2007,** *17* (8), 383-93.
6. Meller, N.; Merlot, S.; Guda, C., CZH proteins: a new family of Rho-GEFs. *J Cell Sci* **2005,** *118* (Pt 21), 4937-46.
7. Cote, J. F.; Motoyama, A. B.; Bush, J. A.; Vuori, K., A novel and evolutionarily conserved PtdIns(3,4,5)P3-binding domain is necessary for DOCK180 signalling. *Nat Cell Biol* **2005,** *7* (8), 797-807.
8. Balagopalan, L.; Chen, M. H.; Geisbrecht, E. R.; Abmayr, S. M., The CDM superfamily protein MBC directs myoblast fusion through a mechanism that requires phosphatidylinositol 3,4,5-triphosphate binding but is independent of direct interaction with DCrk. *Mol Cell Biol* **2006,** *26* (24), 9442-55.
9. Tosello-Trampont, A. C.; Kinchen, J. M.; Brugnera, E.; Haney, L. B.; Hengartner, M. O.; Ravichandran, K. S., Identification of two signaling submodules within the CrkII/ELMO/Dock180 pathway regulating engulfment of apoptotic cells. *Cell Death Differ* **2007,** *14* (5), 963-72.
10. Brugnera, E.; Haney, L.; Grimsley, C.; Lu, M.; Walk, S. F.; Tosello-Trampont, A. C.; Macara, I. G.; Madhani, H.; Fink, G. R.; Ravichandran, K. S., Unconventional Rac-GEF activity is mediated through the Dock180-ELMO complex. *Nat Cell Biol* **2002,** *4* (8), 574-82.
11. Cote, J. F.; Vuori, K., Identification of an evolutionarily conserved superfamily of DOCK180-related proteins with guanine nucleotide exchange activity. *J Cell Sci* **2002,** *115* (Pt 24), 4901-13.
12. Lu, M.; Kinchen, J. M.; Rossman, K. L.; Grimsley, C.; Hall, M.; Sondek, J.; Hengartner, M. O.; Yajnik, V.; Ravichandran, K. S., A Steric-inhibition model for regulation of nucleotide exchange via the Dock180 family of GEFs. *Curr Biol* **2005,** *15* (4), 371-7.
13. Katoh, H.; Negishi, M., RhoG activates Rac1 by direct interaction with the Dock180-binding protein Elmo. *Nature* **2003,** *424* (6947), 461-4.
14. Lu, M.; Kinchen, J. M.; Rossman, K. L.; Grimsley, C.; deBakker, C.; Brugnera, E.; Tosello-Trampont, A. C.; Haney, L. B.; Klingele, D.; Sondek, J.; Hengartner, M. O.; Ravichandran, K. S., PH domain of ELMO functions in trans to regulate Rac activation via Dock180. *Nat Struct Mol Biol* **2004,** *11* (8), 756-62.

15. Gumienny, T. L.; Brugnera, E.; Tosello-Trampont, A. C.; Kinchen, J. M.; Haney, L. B.; Nishiwaki, K.; Walk, S. F.; Nemergut, M. E.; Macara, I. G.; Francis, R.; Schedl, T.; Qin, Y.; Van Aelst, L.; Hengartner, M. O.; Ravichandran, K. S., CED-12/ELMO, a novel member of the CrkII/Dock180/Rac pathway, is required for phagocytosis and cell migration. *Cell* **2001,** *107* (1), 27-41; Wu, Y. C.; Horvitz, H. R., C. elegans phagocytosis and cell-migration protein CED-5 is similar to human DOCK180. *Nature* **1998,** *392* (6675), 501-4; Zhou, Z.; Caron, E.; Hartwieg, E.; Hall, A.; Horvitz, H. R., The C. elegans PH domain protein CED-12 regulates cytoskeletal reorganization via a Rho/Rac GTPase signaling pathway. *Dev Cell* **2001,** *1* (4), 477-89.
16. deBakker, C. D.; Haney, L. B.; Kinchen, J. M.; Grimsley, C.; Lu, M.; Klingele, D.; Hsu, P. K.; Chou, B. K.; Cheng, L. C.; Blangy, A.; Sondek, J.; Hengartner, M. O.; Wu, Y. C.; Ravichandran, K. S., Phagocytosis of apoptotic cells is regulated by a UNC-73/TRIO-MIG-2/RhoG signaling module and armadillo repeats of CED-12/ELMO. *Curr Biol* **2004,** *14* (24), 2208-16.
17. Grimsley, C. M.; Kinchen, J. M.; Tosello-Trampont, A. C.; Brugnera, E.; Haney, L. B.; Lu, M.; Chen, Q.; Klingele, D.; Hengartner, M. O.; Ravichandran, K. S., Dock180 and ELMO1 proteins cooperate to promote evolutionarily conserved Rac-dependent cell migration. *J Biol Chem* **2004,** *279* (7), 6087-97.
18.Komander, D.; Patel, M.; Laurin, M.; Fradet, N.; Pelletier, A.; Barford, D.; Cote, J. F., An alpha-helical extension of the ELMO1 pleckstrin homology domain mediates direct interaction to DOCK180 and is critical in Rac signaling. *Mol Biol Cell* **2008,** *19* (11), 4837-51.
19. Duchek, P.; Somogyi, K.; Jekely, G.; Beccari, S.; Rorth, P., Guidance of cell migration by the Drosophila PDGF/VEGF receptor. *Cell* **2001,** *107* (1), 17-26.
20. Erickson, M. R.; Galletta, B. J.; Abmayr, S. M., Drosophila myoblast city encodes a conserved protein that is essential for myoblast fusion, dorsal closure, and cytoskeletal organization. *J Cell Biol* **1997,** *138* (3), 589-603.
21. Geisbrecht, E. R.; Haralalka, S.; Swanson, S. K.; Florens, L.; Washburn, M. P.; Abmayr, S. M., Drosophila ELMO/CED-12 interacts with Myoblast city to direct myoblast fusion and ommatidial organization. *Dev Biol* **2008,** *314* (1), 137-49.
22. Ishimaru, S.; Ueda, R.; Hinohara, Y.; Ohtani, M.; Hanafusa, H., PVR plays a critical role via JNK activation in thorax closure during Drosophila metamorphosis. *EMBO J* **2004,** *23* (20), 3984-94.
23. Hakeda-Suzuki, S.; Ng, J.; Tzu, J.; Dietzl, G.; Sun, Y.; Harms, M.; Nardine, T.; Luo, L.; Dickson, B. J., Rac function and regulation during Drosophila development. *Nature* **2002,** *416* (6879), 438-42.
24. Luo, L.; Liao, Y. J.; Jan, L. Y.; Jan, Y. N., Distinct morphogenetic functions of similar small GTPases: Drosophila Drac1 is involved in axonal outgrowth and myoblast fusion. *Genes Dev* **1994,** *8* (15), 1787-802; Ng, J.; Nardine, T.; Harms, M.; Tzu, J.; Goldstein, A.; Sun, Y.; Dietzl, G.; Dickson, B. J.; Luo, L., Rac GTPases control axon growth, guidance and branching. *Nature* **2002,** *416* (6879), 442-7.
25.Nolan, K. M.; Barrett, K.; Lu, Y.; Hu, K. Q.; Vincent, S.; Settleman, J., Myoblast city, the Drosophila homolog of DOCK180/CED-5, is required in a Rac signaling pathway utilized for multiple developmental processes. *Genes Dev* **1998,** *12* (21), 3337-42.
26. Yajnik, V.; Paulding, C.; Sordella, R.; McClatchey, A. I.; Saito, M.; Wahrer, D. C.; Reynolds, P.; Bell, D. W.; Lake, R.; van den Heuvel, S.; Settleman, J.; Haber, D. A.,

DOCK4, a GTPase activator, is disrupted during tumorigenesis. *Cell* **2003,** *112* (5), 673-84.
27. Pannekoek, W. J.; Kooistra, M. R.; Zwartkruis, F. J.; Bos, J. L., Cell-cell junction formation: the role of Rap1 and Rap1 guanine nucleotide exchange factors. *Biochim Biophys Acta* **2009,** *1788* (4), 790-6.
28. Eguchi, K.; Yoshioka, Y.; Yoshida, H.; Morishita, K.; Miyata, S.; Hiai, H.; Yamaguchi, M., The Drosophila DOCK family protein sponge is involved in differentiation of R7 photoreceptor cells. *Exp Cell Res* **2013,** *319* (14), 2179-95.
29. Biersmith, B.; Liu, Z. C.; Bauman, K.; Geisbrecht, E. R., The DOCK protein sponge binds to ELMO and functions in Drosophila embryonic CNS development. *PLoS One* **2011,** *6* (1), e16120.
30. Ueda, S.; Negishi, M.; Katoh, H., Rac GEF Dock4 interacts with cortactin to regulate dendritic spine formation. *Mol Biol Cell* **2013,** *24* (10), 1602-13.
31. Kang, H.; Davis-Dusenbery, B. N.; Nguyen, P. H.; Lal, A.; Lieberman, J.; Van Aelst, L.; Lagna, G.; Hata, A., Bone morphogenetic protein 4 promotes vascular smooth muscle contractility by activating microRNA-21 (miR-21), which down-regulates expression of family of dedicator of cytokinesis (DOCK) proteins. *J Biol Chem* **2012,** *287* (6), 3976-86.
32. Namekata, K.; Kimura, A.; Kawamura, K.; Harada, C.; Harada, T., Dock GEFs and their therapeutic potential: Neuroprotection and axon regeneration. *Prog Retin Eye Res* **2014**, *43*, (1), 1-16.
33. Bianco, A.; Poukkula, M.; Cliffe, A.; Mathieu, J.; Luque, C. M.; Fulga, T. A.; Rørth, P., Two distinct modes of guidance signalling during collective migration of border cells. *Nature* **2007,** *448* (7151), 362-5.
34. Washburn, M. P.; Wolters, D.; Yates, J. R., 3rd, Large-scale analysis of the yeast proteome by multidimensional protein identification technology. *Nat Biotechnol* **2001,** *19* (3), 242-7.
35. Rice, T. B.; Garen, A., Localized defects of blastoderm formation in maternal effect mutants of Drosophila. *Dev Biol* **1975,** *43* (2), 277-86.
36. Postner, M. A.; Miller, K. G.; Wieschaus, E. F., Maternal effect mutations of the sponge locus affect actin cytoskeletal rearrangements in Drosophila melanogaster embryos. *J Cell Biol* **1992,** *119* (5), 1205-18.
37. Bianco, A.; Poukkula, M.; Cliffe, A.; Mathieu, J.; Luque, C. M.; Fulga, T. A.; Rorth, P., Two distinct modes of guidance signalling during collective migration of border cells. *Nature* **2007,** *448* (7151), 362-5.
38. Lu, M. a. R., K, Activation of GTPases by Dock180 family of proteins. In *Rho Family GTPases*, 2005; pp 73-92.
39. Hiramoto, K.; Negishi, M.; Katoh, H., Dock4 is regulated by RhoG and promotes Rac-dependent cell migration. *Exp Cell Res* **2006,** *312* (20), 4205-16.
40. Brody, T.; Stivers, C.; Nagle, J.; Odenwald, W. F., Identification of novel Drosophila neural precursor genes using a differential embryonic head cDNA screen. *Mech Dev* **2002,** *113* (1), 41-59.
41. Hayashi, S.; Rubinfeld, B.; Souza, B.; Polakis, P.; Wieschaus, E.; Levine, A. J., A Drosophila homolog of the tumor suppressor gene adenomatous polyposis coli down-regulates beta-catenin but its zygotic expression is not essential for the regulation of Armadillo. *Proc Natl Acad Sci U S A* **1997,** *94* (1), 242-7.

42. Chen, Q.; Chen, T. J.; Letourneau, P. C.; Costa Lda, F.; Schubert, D., Modifier of cell adhesion regulates N-cadherin-mediated cell-cell adhesion and neurite outgrowth. *J Neurosci* **2005,** *25* (2), 281-90.
43. Iwai, Y.; Usui, T.; Hirano, S.; Steward, R.; Takeichi, M.; Uemura, T., Axon patterning requires DN-cadherin, a novel neuronal adhesion receptor, in the Drosophila embryonic CNS. *Neuron* **1997,** *19* (1), 77-89.
44. Prakash, S.; Caldwell, J. C.; Eberl, D. F.; Clandinin, T. R., Drosophila N-cadherin mediates an attractive interaction between photoreceptor axons and their targets. *Nat Neurosci* **2005,** *8* (4), 443-50.
45. Goicoechea, S. M.; Awadia, S.; Garcia-Mata, R., I'm coming to GEF you: Regulation of RhoGEFs during cell migration. *Cell Adh Migr* **2014,** *8* (4); Tetlow, A. L.; Tamanoi, F., The Ras superfamily G-proteins. *Enzymes* **2013,** *33 Pt A*, 1-14.
46. Cook, D. R.; Rossman, K. L.; Der, C. J., Rho guanine nucleotide exchange factors: regulators of Rho GTPase activity in development and disease. *Oncogene* **2014,** *33* (31), 4021-35.
47. Rossman, K. L.; Der, C. J.; Sondek, J., GEF means go: turning on RHO GTPases with guanine nucleotide-exchange factors. *Nat Rev Mol Cell Biol* **2005,** *6* (2), 167-80.
48.Komander, D.; Patel, M.; Laurin, M.; Fradet, N.; Pelletier, A.; Barford, D.; Côté, J. F., An alpha-helical extension of the ELMO1 pleckstrin homology domain mediates direct interaction to DOCK180 and is critical in Rac signaling. *Mol Biol Cell* **2008,** *19* (11), 4837-51.
49. Laurin, M.; Fradet, N.; Blangy, A.; Hall, A.; Vuori, K.; Côté, J. F., The atypical Rac activator Dock180 (Dock1) regulates myoblast fusion in vivo. *Proc Natl Acad Sci U S A* **2008,** *105* (40), 15446-51.
50. Li, X.; Gao, X.; Liu, G.; Xiong, W.; Wu, J.; Rao, Y., Netrin signal transduction and the guanine nucleotide exchange factor DOCK180 in attractive signaling. *Nat Neurosci* **2008,** *11* (1), 28-35.
51. Sanematsu, F.; Hirashima, M.; Laurin, M.; Takii, R.; Nishikimi, A.; Kitajima, K.; Ding, G.; Noda, M.; Murata, Y.; Tanaka, Y.; Masuko, S.; Suda, T.; Meno, C.; Côté, J. F.; Nagasawa, T.; Fukui, Y., DOCK180 is a Rac activator that regulates cardiovascular development by acting downstream of CXCR4. *Circ Res* **2010,** *107* (9), 1102-5; Tachibana, K.; Hirota, S.; Iizasa, H.; Yoshida, H.; Kawabata, K.; Kataoka, Y.; Kitamura, Y.; Matsushima, K.; Yoshida, N.; Nishikawa, S.; Kishimoto, T.; Nagasawa, T., The chemokine receptor CXCR4 is essential for vascularization of the gastrointestinal tract. *Nature* **1998,** *393* (6685), 591-4; Moore, C. A.; Parkin, C. A.; Bidet, Y.; Ingham, P. W., A role for the Myoblast city homologues Dock1 and Dock5 and the adaptor proteins Crk and Crk-like in zebrafish myoblast fusion. *Development* **2007,** *134* (17), 3145-53.
52. Chen, Q.; Chen, T. J.; Letourneau, P. C.; Costa, L. a. F.; Schubert, D., Modifier of cell adhesion regulates N-cadherin-mediated cell-cell adhesion and neurite outgrowth. *J Neurosci* **2005,** *25* (2), 281-90.
53. Chen, Q.; Peto, C. A.; Shelton, G. D.; Mizisin, A.; Sawchenko, P. E.; Schubert, D., Loss of modifier of cell adhesion reveals a pathway leading to axonal degeneration. *J Neurosci* **2009,** *29* (1), 118-30.
54. Pagnamenta, A. T.; Bacchelli, E.; de Jonge, M. V.; Mirza, G.; Scerri, T. S.; Minopoli, F.; Chiocchetti, A.; Ludwig, K. U.; Hoffmann, P.; Paracchini, S.; Lowy, E.; Harold, D. H.; Chapman, J. A.; Klauck, S. M.; Poustka, F.; Houben, R. H.; Staal, W. G.; Ophoff, R.

A.; O'Donovan, M. C.; Williams, J.; Nöthen, M. M.; Schulte-Körne, G.; Deloukas, P.; Ragoussis, J.; Bailey, A. J.; Maestrini, E.; Monaco, A. P.; Consortium, I. M. G. S. O. A., Characterization of a family with rare deletions in CNTNAP5 and DOCK4 suggests novel risk loci for autism and dyslexia. *Biol Psychiatry* **2010,** *68* (4), 320-8; Shi, L., Dock protein family in brain development and neurological disease. *Commun Integr Biol* **2013,** *6* (6), e26839.
55. Erickson, M. R.; Galletta, B. J.; Abmayr, S. M., Drosophila myoblast city encodes a conserved protein that is essential for myoblast fusion, dorsal closure, and cytoskeletal organization. *J Cell Biol* **1997,** *138* (3), 589-603.
56. Duchek, P.; Somogyi, K.; Jékely, G.; Beccari, S.; Rørth, P., Guidance of cell migration by the Drosophila PDGF/VEGF receptor. *Cell* **2001,** *107* (1), 17-26.
57. Balagopalan, L.; Chen, M. H.; Geisbrecht, E. R.; Abmayr, S. M., The CDM superfamily protein MBC directs myoblast fusion through a mechanism that requires phosphatidylinositol 3,4,5-triphosphate binding but is independent of direct interaction with DCrk. *Mol Cell Biol* **2006,** *26* (24), 9442-55.
58. Abmayr, S. M.; Pavlath, G. K., Myoblast fusion: lessons from flies and mice. *Development* **2012,** *139* (4), 641-56.
59. Haralalka, S.; Abmayr, S. M., Myoblast fusion in Drosophila. *Exp Cell Res* **2010,** *316* (18), 3007-13.
60. Haralalka, S.; Shelton, C.; Cartwright, H. N.; Katzfey, E.; Janzen, E.; Abmayr, S. M., Asymmetric Mbc, active Rac1 and F-actin foci in the fusion-competent myoblasts during myoblast fusion in Drosophila. *Development* **2011,** *138* (8), 1551-62.
61. Tao, Y.; Schulz, R. A., Heart development in Drosophila. *Semin Cell Dev Biol* **2007,** *18* (1), 3-15; Singh, A.; Irvine, K. D., Drosophila as a model for understanding development and disease. *Dev Dyn* **2012,** *241* (1), 1-2.
62. Haag, T. A.; Haag, N. P.; Lekven, A. C.; Hartenstein, V., The role of cell adhesion molecules in Drosophila heart morphogenesis: faint sausage, shotgun/DE-cadherin, and laminin A are required for discrete stages in heart development. *Dev Biol* **1999,** *208* (1), 56-69.
63. Santiago-Martínez, E.; Soplop, N. H.; Patel, R.; Kramer, S. G., Repulsion by Slit and Roundabout prevents Shotgun/E-cadherin-mediated cell adhesion during Drosophila heart tube lumen formation. *J Cell Biol* **2008,** *182* (2), 241-8.
64. Medioni, C.; Astier, M.; Zmojdzian, M.; Jagla, K.; Sémériva, M., Genetic control of cell morphogenesis during Drosophila melanogaster cardiac tube formation. *J Cell Biol* **2008,** *182* (2), 249-61.
65.Helenius, I. T.; Beitel, G. J., The first "Slit" is the deepest: the secret to a hollow heart. *J Cell Biol* **2008,** *182* (2), 221-3; Medioni, C.; Sénatore, S.; Salmand, P. A.; Lalevée, N.; Perrin, L.; Sémériva, M., The fabulous destiny of the Drosophila heart. *Curr Opin Genet Dev* **2009,** *19* (5), 518-25.
66. Yajnik, V.; Paulding, C.; Sordella, R.; McClatchey, A. I.; Saito, M.; Wahrer, D. C.; Reynolds, P.; Bell, D. W.; Lake, R.; van den Heuvel, S.; Settleman, J.; Haber, D. A., DOCK4, a GTPase activator, is disrupted during tumorigenesis. *Cell* **2003,** *112* (5), 673-84.
67. Ueda, S.; Fujimoto, S.; Hiramoto, K.; Negishi, M.; Katoh, H., Dock4 regulates dendritic development in hippocampal neurons. *J Neurosci Res* **2008,** *86* (14), 3052-61.

68. Yan, D.; Li, F.; Hall, M. L.; Sage, C.; Hu, W. H.; Giallourakis, C.; Upadhyay, G.; Ouyang, X. M.; Du, L. L.; Bethea, J. R.; Chen, Z. Y.; Yajnik, V.; Liu, X. Z., An isoform of GTPase regulator DOCK4 localizes to the stereocilia in the inner ear and binds to harmonin (USH1C). *J Mol Biol* **2006,** *357* (3), 755-64.
69. Awasaki, T.; Saito, M.; Sone, M.; Suzuki, E.; Sakai, R.; Ito, K.; Hama, C., The Drosophila trio plays an essential role in patterning of axons by regulating their directional extension. *Neuron* **2000,** *26* (1), 119-31.
70. Bateman, J.; Shu, H.; Van Vactor, D., The guanine nucleotide exchange factor trio mediates axonal development in the Drosophila embryo. *Neuron* **2000,** *26* (1), 93-106; Fritz, J. L.; VanBerkum, M. F., Calmodulin and son of sevenless dependent signaling pathways regulate midline crossing of axons in the Drosophila CNS. *Development* **2000,** *127* (9), 1991-2000; Liebl, E. C.; Forsthoefel, D. J.; Franco, L. S.; Sample, S. H.; Hess, J. E.; Cowger, J. A.; Chandler, M. P.; Shupert, A. M.; Seeger, M. A., Dosage-sensitive, reciprocal genetic interactions between the Abl tyrosine kinase and the putative GEF trio reveal trio's role in axon pathfinding. *Neuron* **2000,** *26* (1), 107-18.
71. Yang, L.; Bashaw, G. J., Son of sevenless directly links the Robo receptor to rac activation to control axon repulsion at the midline. *Neuron* **2006,** *52* (4), 595-607.
72. Medley, Q. G.; Buchbinder, E. G.; Tachibana, K.; Ngo, H.; Serra-Pages, C.; Streuli, M., Signaling between focal adhesion kinase and trio. *J Biol Chem* **2003,** *278* (15), 13265-70.
73. Forsthoefel, D. J.; Liebl, E. C.; Kolodziej, P. A.; Seeger, M. A., The Abelson tyrosine kinase, the Trio GEF and Enabled interact with the Netrin receptor Frazzled in Drosophila. *Development* **2005,** *132* (8), 1983-94.
74. Round, J.; Stein, E., Netrin signaling leading to directed growth cone steering. *Curr Opin Neurobiol* **2007,** *17* (1), 15-21.
75. Makino, Y.; Tsuda, M.; Ichihara, S.; Watanabe, T.; Sakai, M.; Sawa, H.; Nagashima, K.; Hatakeyama, S.; Tanaka, S., Elmo1 inhibits ubiquitylation of Dock180. *J Cell Sci* **2006,** *119* (Pt 5), 923-32.
76. Kiyokawa, E.; Hashimoto, Y.; Kurata, T.; Sugimura, H.; Matsuda, M., Evidence that DOCK180 up-regulates signals from the CrkII-p130(Cas) complex. *J Biol Chem* **1998,** *273* (38), 24479-84.
77. Yokoyama, N.; deBakker, C. D.; Zappacosta, F.; Huddleston, M. J.; Annan, R. S.; Ravichandran, K. S.; Miller, W. T., Identification of tyrosine residues on ELMO1 that are phosphorylated by the Src-family kinase Hck. *Biochemistry* **2005,** *44* (24), 8841-9.
78. Côté, J. F.; Vuori, K., Identification of an evolutionarily conserved superfamily of DOCK180-related proteins with guanine nucleotide exchange activity. *J Cell Sci* **2002,** *115* (Pt 24), 4901-13.
79. Namekata, K.; Enokido, Y.; Iwasawa, K.; Kimura, H., MOCA induces membrane spreading by activating Rac1. *J Biol Chem* **2004,** *279* (14), 14331-7.
80. Yang, J.; Zhang, Z.; Roe, S. M.; Marshall, C. J.; Barford, D., Activation of Rho GTPases by DOCK exchange factors is mediated by a nucleotide sensor. *Science* **2009,** *325* (5946), 1398-402.

VITA

Bridget Hope Biersmith graduated in 2008 from the University of Missouri - Kansas City with a Bachelor of Science in Biology. Following this, she worked as an research assistant in the lab of Dr. Lenoard Dobens at the University of Missouri - Kansas City. From 2009 – 2010 she was a laboratory technician for Dr. Erika Geisbrecht at UMKC. In 2009, she started her Interdisciplinary Doctor of Philosophy degree in Cell Biolgy & Biophysics and Molecular Biology & Biochemistry. During her graduate career, she published 3 first author papers and obtained a grant from the American Heart Association. Her work focused on the role of two conserved Dock proteins; Myoblast City and Sponge. She established the two do not function redundantly in the development of the *Drosophila* central nervous system, somatic muscle, and dorsal vessel. In December of 2014, she was granted her doctorate degree for her work titled "Determining the Differential Roles of the Dock Family of GEFs in *Drosophila* Development."